Resilient Provision of Ecosystem Services from Agricultural Landscapes: Tradeoffs Involving Means and Variances of Water Quality Improvements

ABSTRACT

We assess the tradeoffs and synergies involved in reducing agriculture-generated nutrient loads with different levels of resilience. We optimize the selection of least-cost patterns of agricultural conservation practices for both the expected performance of the conservation actions and its variance. Securing nutrient loads with a higher level of resilience is costly, with marginal costs of resilience generally declining with lower loads. We find that the main tradeoff dimension is between cost of conservation investments and ecosystem service objectives, as opposed to pronounced mean-variance or between- nutrient objectives tradeoffs. We find relative synergies in agricultural conservation investments aimed at nutrient reductions.

Keywords: *agricultural conservation practices, agricultural nonpoint-source pollution, ecosystem services tradeoffs; multiobjective optimization; evolutionary algorithms, safety-first; resilience*

JEL Codes: Q25, C63

Suggested running head: Resilient Provision of Water Quality from Agriculture

Sergey Rabotyagov (corresponding author),
Associate Professor
School of Environmental and Forest Sciences,
Box 352100,
University of Washington, Seattle WA 98195-2100
Tel: 515-451-7218
Fax: 206-685-0790
E-mail: *rabotyag@uw.edu*

Adriana Valcu
Postdoctoral Research Associate
Center for Agricultural and Rural Development
Department of Economics
Iowa State University, Ames, IA

Catherine L. Kling
Director and Charles F. Curtiss Distinguished Professor
Center for Agricultural and Rural Development
Department of Economics
Iowa State University, Ames, IA

Acknowledgments

This research was funded in part from support received from the National Science Foundation's Water, Sustainability, and Climate program joint with National Institute of Food and Agriculture (#NSF-WSC 1209402 and WNZ-A71219) and two awards from the National Institute of Food and Agriculture (#2014-51130-22494 and 2011-68002-30190).

We thank Todd Campbell, Phil Gassman, and Yongjie Ji for technical assistance and helpful suggestions. All errors remain our sole responsibility.

Resilient Provision of Ecosystem Services from Agricultural Landscapes: Tradeoffs Involving Means and Variances of Water Quality Improvements

Longer abstract

Many ecosystem services are rival and important tradeoffs exist in their production process, while some jointness in production (synergies) are also postulated to exist. We assess the strength of tradeoffs and synergies involved in reducing agriculture-generated watershed nutrient loads with different levels of resilience. We define resilience as the simulated probability of attaining the desired level of nutrient load. We spatially optimize the selection of least-cost patterns of agricultural conservation practices or both the expected performance of the conservation actions and its variance. The modeling framework is applied to the Boone River Watershed in Iowa. The empirical results confirm that securing nutrient loads with a higher level of resilience is costly. However, the marginal cost is not necessarily increasing: focusing on larger nutrient reductions allows one to obtain resilience at a smaller additional cost than if one is seeking only modest nutrient reductions. In our model, this is due to the ability of perennial grassland to buffer against exogenous shocks and to drastically reduce variability in nutrient loads. In extending the model to two nutrients, nitrogen and phosphorus, we find that the main tradeoff dimension is between cost of conservation investments and ecosystem service objectives, as opposed to pronounced mean-variance tradeoffs or strong tradeoffs between the two nutrient objectives. While some meaningful tradeoffs exist between nutrient objectives, our findings highlight the presence of relative synergies in agricultural conservation investments aimed at nutrient reductions. However, while *relative* synergies exist, controlling risk of nutrient loads is once again shown to have high opportunity costs, and resilience comes at a significant premium.

In recent years, the concept of ecosystem services and natural capital has garnered significant attention from the research, policy, and conservation community (see, e.g., Heal and Small (2002), Boyd and Banzhaf (2007), Polasky and Segerson (2009), Barbier (2015), and a Special Feature in the *Proceedings of National Academy of Sciences* devoted to the topic). For intensively managed agriculture-dominated landscapes, there can be both complementarities and competition between ecosystem services including the provisioning services of food, feed, fuel, and clean water, the regulating service of waste processing (provided by streams), and the cultural ecosystem services tied to the presence of wildlife for hunting or recreation. The diminution of ecosystem services related to environmental externalities is, of course, a generally expected outcome of a market system. Given the signals provided by agricultural markets, it is not surprising that the agricultural system heavily favors production of private ecosystem services (food, feed, and fuel) (Lichtenberg 2002, p. 1254). The US Midwest, for example, has the highest rates of crop growth in the world, to the point that agriculture affects regional climate (Mueller et al. 2015). At the same time, heavy reliance on fertilizer use, has caused some scientists to suggest that humanity has exceeded its "safe operating space" with respect to nutrient fluxes (Steffen et al. 2015).

The recognition of these issues has led to extensive agri-environmental policy efforts in the US and elsewhere as well as a literature identifying approaches for incorporating ecological objectives in policy (Lichtenberg 2002; Lankoski and Ollikainen 2003, Bateman et al. 2013). While these efforts have found some success, most scientific assessments of environmental impacts of U.S. agriculture indicate many remaining concerns including fish and wildlife habitat (USDA-CEAP, Wildlife National Assessment 2015), air pollution (Mueller and Mendelsohn 2011), nutrient pollution (US EPA 2015), and other environmental endpoints.

Elucidating the nature of tradeoffs between different ecosystem services requires understanding natural system processes and evaluating *counterfactual* scenarios to determine where tradeoffs exist, where synergies occur (e.g., Karp et al. 2015), and how other ecosystem services can be improved at the lowest sacrifice to marketed agricultural goods. Understanding tradeoffs or potential synergies[1] requires two things. First is the quantifiable understanding of the underlying ecosystem service production process and of the economic inputs that go into their production.[2] The ecological production functions themselves, however, are often poorly understood, may exhibit complex nonlinear dynamics with thresholds (e.g., Carpenter et al. 2015; Barbier et al. 2008), or, even in the best case of relatively small scientific uncertainty, may be represented by computer simulation programs that do not correspond to traditional economics understanding of a production function (e.g., Heal and Small 2002).

While tradeoffs in ecosystem services may be unavoidable, it is desirable to limit consideration to those that are on a Pareto-efficient frontier. This is particularly important when considering the exact magnitudes (marginal costs or marginal rates of product transformation) of tradeoffs between ecosystem services. Yet another dimension to the question of tradeoffs between different classes of ecosystem services is uncertainty in the provision of a particular joint product from an ecosystem. In addition to having different opportunity costs of private goods, alternative ecosystem service bundle can differ in terms of the risk associated with their provision. That is, some conservation investments may consistently yield a given bundle of ecosystem services while others may on average a higher level of services, but with a wider

[1] Heal et al. (2001) called the presence of synergies a "conservation umbrella."

[2] See Heal and Small (2002) for an interesting distinction between economic and non-economic inputs into the ecosystem services production function. Economic inputs have opportunity costs, while others, like sunlight needed for agricultural production, while essential, are non-economic In our application, economic inputs include foregoing crop production entirely and planting perennial grass or bringing machinery, expertise, and labor inputs for the adoption of "working land" conservation practices.

128 variability of provision over time. The mean-variance tradeoff for a particular cost of
129 conservation investment may be relevant in choosing across services.

130 Consideration of tradeoffs between mean and variance of provision of services is
131 consistent with the literature on resilience in ecosystem service provision. The notion of
132 resilience is nuanced and complex, but for this work we adopt a definition similar to one used in
133 Gren (2010) —namely, the reliability of ecosystem service provision under exogenous shocks,
134 specifically weather risk.[3] In this paper, we explore tradeoffs for the expected provision level and
135 for different levels of reliability (specified as simulated probability of attaining the desired
136 provision level) for the case of a single non-market ecosystem service, and then expand the
137 notion of tradeoffs to multiple dimensions of aquatic ecosystem services, where we focus on the
138 joint probability of meeting desired ecological targets.[4] To do so, we adopt a multiobjective
139 optimization approach with the objectives specified as means and standard deviations of desired
140 ecosystem outputs. For this application, we focus on a heavily agricultural watershed in Iowa and
141 use nutrient loads as inputs into aquatic ecosystem services. This approach can will be relevant to
142 any situation where the connection between human actions on the landscape and ecosystem
143 services is characterized by a complex relationship involving nonlinearities, nonconvexities and
144 nonseparabilities (for example, conservation network design as in Parkhurst and Shogren 2008).

145

[3] Social preference for reliability of goal attainment is reflected in the required "margin of safety" in the TMDL regulations, requiring either to explicitly reduce allowable pollutant loads in a watershed based on modeled uncertainty or to employ conservative modeling assumptions (http://water.epa.gov/lawsregs/lawsguidance/cwa/tmdl/TMDL-ch3.cfm)

[4] However, as Heal and Small (2002) point out "We are powerfully ignorant about the technology that produces ecosystem services." While true, ignorance should not be a reason to explore the implications of existing levels of understanding of some dimensions of ecosystem services production process, embodied, in our case, in the ecohydrologic model. See Kling (2011) for a call to action while acknowledging the deep uncertainties involved and importance of learning and adaptive management.
.

Resilience in ecosystem services provision

The concept of resilience has been used extensively by many disciplines, each approaching the concept from somewhat different perspectives and providing different definitions. We refer the reader to Longstaff et al.'s (2013) typology and to translate the concept among different disciplines. Intuitively, the notion of resilience deals with the ability of a system to perform desired functions under most, if not all, possible external shocks. Within their typology, we adopt the definition referred to as Type I resilience: the capacity of a system "to rebound and recover." Simply put, we seek to spatially optimize the selection of agricultural conservation practices which optimize both the expected performance of the conservation actions and their variance (Shortle and Horan (2013) suggest a similar approach). Longstaff et al's (2013) typology distinguishes approaches to resilience based on level of complexity (low/reductionist approach to high/holism/emergent properties) of the studied system as well as based on degree of normativity (on the scale from descriptive/positive to normative). Our work fits in the low complexity/low normativity category, as our studied system deals with quantifiable uncertainty (risk) and employs a deterministic, reductionist approach to quantifying the costs and ecosystem service outputs of evaluated scenarios.[5] This definition of resilience can be equivalently thought of as the reliability of meeting ecosystem service provision targets.

Next, we briefly sketch a simple model to aid in conceptual framing of our work. Suppose one possesses a quantified joint ecological-economic production function $S(\boldsymbol{x};\boldsymbol{\varepsilon})$: $\mathbb{R}^{\boldsymbol{m}} \rightarrow \mathbb{R}^{\boldsymbol{k}}$, where $\boldsymbol{x}$ is an $m \times 1$ vector of controllable economic inputs into the production of ecosystem services (e.g., land, machinery, labor, fertilizer input, conservation

[5] Were we to adopt a specific form for an economic damage function associated with ecosystem service degradation, our work would align with type II resilience definition of Longstaff et al. (2013), and would involve objectives of net benefit optimization (see Polasky and Segerson (2009) and Shortle and Horan (2013) for discussion of the relationship between outcomes obtained under physically defined goals and economically efficient outcomes).

practices) being combined, over the relevant spatial and temporal scale, to produce a $k \times 1$ vector of monetized benefits/costs and nonmonetized final ecosystem services, and $\boldsymbol{\varepsilon}$ representing exogenous factors (e.g., non-economic inputs into production of ecosystem services such as rainfall, solar radiation, soil quality, as well as exogenous economic factors such as commodity prices or government policy) treated as random. One of the components of the output vector serves to monetize the choices made with respect to human actions $\boldsymbol{x}$ in the form of net social benefits. Depending on the availability of data and models, this can range from a full accounting of net social benefits measuring welfare impacts of marketed ecosystem services and non-market values of some non-market ecosystem services to simply measuring estimated engineering costs associated with $\boldsymbol{x}$. With this resilience measure, it is assumed that decision-makers can specify a set of desirable performance targets $\bar{S}$. Appropriately scaling outputs so that they are all desirable, the problem of resilience can be written as $\max_{\boldsymbol{x}} P(S(\boldsymbol{x};\boldsymbol{\varepsilon}) \geq \bar{S})$, that is, the most resilient set of actions are those that maximize the probability of meeting a desired level of monetized and non-monetized ecosystem services.

This is a version of Roy's (1952) safety-first criterion.[6] Safety-first approaches have found numerous applications in many fields, including agricultural and environmental economics. Of many past efforts, examples include Paris (1979), Beavis and Walker (1983), Lichtenberg and Zilberman (1988), McSweeny and Shortle (1990), Bigman (1996), Willis and Whittlesey (1998), Horan and Shortle (2011), Eloffson (2003), Gren (2008), Kampas and White (2003), Rabotyagov (2010). As highlighted by Shortle and Horan (2013), the Total Maximum Daily Load rules adopts safety-first approach through the requirement of a "margin of safety"

[6] More broadly, this kind of formulation can be described as a P-model of Chance-Constrained Programming (CCP) of Charnes and Cooper (1959), and CCP can be described as a class of anticipative (non-adaptive) stochastic programming approaches (Poojari and Varghese 2008)

188 constraint on the allowable watershed pollution loads. Another example is that the government of
189 Canada was at one point explicitly favoring climate change policy requiring 95% certainty in
190 agricultural carbon sequestration credits (Rabotyagov 2010).

191 In many applications, the tradeoffs embedded in resilience can be appropriately
192 formulated by minimizing the (non-stochastic) cost of achieving a single stochastic ecosystem
193 service objective with a given probability. The resilience objective is typically written as a
194 constraint $P(S_i(\boldsymbol{x};\boldsymbol{\varepsilon}) \geq \bar{S_i}) \geq \alpha$, where α is level of resilience (or reliability) of the system.
195 Rewriting the probabilistic constraint in a deterministic form can be accomplished when the
196 distribution of the random term is known. In this case, a deterministic constraint involving the
197 critical value of the standardized distribution of S_i, the controlled mean and variance of
198 ecosystem service provision can be written as $E_\varepsilon\big(S_i(\boldsymbol{x})\big) + F_z^{-1}(1-\alpha)Var\big(S_i(\boldsymbol{x})\big)^{0.5} \geq \bar{S_i}$.
199 For high desired levels of confidence α (so that $F_z^{-1}(1-\alpha) < 0$), the term ($F_z^{-1}(1-$
200 $\alpha)Var\big(S_i(\boldsymbol{x})\big)^{0.5}$) has the standard interpretation of a "margin of safety" or of an "uncertainty
201 discount". Tradeoffs between costs and the resilience of providing non-monetized ecosystem
202 services are then seen by increasing cost of attaining higher reliability. This is a standard finding,
203 although the costs of resilience have varied from single-digit percentage uncertainty discounts
204 for soil carbon sequestration (Rabotyagov 2010), to almost doubling the costs of pollution
205 reduction when required confidence in pollution reduction goes from 50 to 90-95% (Bÿstrom,
206 Andersson, Gren (2000); Elofsson (2003)) to finding a seven-fold increase in costs of controlling
207 N runoff (McSweeny and Shortle, 1990). Resilience is costly, but the exact tradeoffs involved in
208 achieving higher resilience depends on the particular situation.[7]

[7] An obvious source of affecting costs of resilience lies with the choice of the critical value $F_z^{-1}(1-\alpha)$. Under uncertainty about the form of the controlled distribution, one can purchase resilience with respect to distributional

The simple case of no uncertainty in the opportunity costs of ecosystem services provision allows for a particularly convenient inversion of the probability statement and for dealing with "resilient" levels of provision. If $\boldsymbol{x}$ is costly, the constraint will be binding and $E_{\varepsilon}\left(S_i(\boldsymbol{x}^*)\right) + F_z^{-1}(1-\alpha)Var\left(S_i(\boldsymbol{x}^*)\right)^{0.5} = \bar{S}_i$ represents the α-quantile of the controlled provision distribution (also sometimes referred to as a claimable amount (Kurkalova 2005)) and $\boldsymbol{x}^*$ denotes choices leading to resilient provision. When multiple objectives are brought under the joint probabilistic constraint, such an inversion from joint probabilities to unique quantiles is no longer possible, except for the case of statistically independent objectives, where the jointly α^n-resilient set is constructed of individual (marginal) α-resilient provision levels. Instead, combinations of individual provision levels which jointly produce the desired α-level resilience will be required. This is akin to confidence ellipses encountered in joint significance testing of regression parameters (for the introduction to the issues encountered in joint chance constraints, see Bawa (1973), Prekopa (1970), Willis and Whittlesey (1998) for an applied agricultural economics example or Hong, Yang, and Zhang (2011) for the modern operations research perspective). In short, a simple interpretation of results as producing unique "resilient" $\bar{S}_i$, $\bar{S}_k$ no longer applies.

Fortunately, if we ask "what is the joint resilience associated with a particular solution $\boldsymbol{x}$ and specified objectives, $\bar{S}$?", the answer, expressed as a joint probability, is easy to understand (if not necessarily compute). Namely, the probability is $P(\boldsymbol{x}) = \int I[S(\boldsymbol{x};\boldsymbol{\varepsilon}) \geq \bar{S}]dF(\varepsilon)$. In some simpler cases, where a single stochastic objective is encountered, and a particular distribution for the random factor (e.g., normal) is assumed, the probability can be retrieved from existing tables.

uncertainty by relying on the Chebyschev Inequality (e.g., Gren (2010)). This, however, appears unnecessarily conservative for most practical applications.

In other cases of intermediate difficulty, in which a low-dimension economic-ecological production process may be assumed to be linear and separable ($S(\boldsymbol{x};\boldsymbol{\varepsilon}) \equiv \boldsymbol{s}(\boldsymbol{\varepsilon})'\boldsymbol{x}$), analytical expressions can be constructed (e.g., (Kampas and White 2003). However, even for a single dimension of ecosystem service output, where the production process may take place over K locations, and where multiple actions (J) are available in $\boldsymbol{x}$, construction of (conditional on $\boldsymbol{x}$) variance to arrive at the standardized ecosystem output involves estimating $\frac{KJ(KJ-1)}{2}$ terms of the variance-covariance matrix, which would account for all the spatial and action-related covariances. This is a common problem that arises in risk management, and analytical techniques such as copula estimation exist to aid researchers and decision-makers (Cherubini, Luciano, and Vecchiato, 2004).

Gren (2010) considered several abatement actions and the implied abatement correlations across actions in estimating the resilience value of wetlands for nutrient reduction; however, her analysis did not incorporate spatial correlations, while Kampas and White (2003) have shown that ignoring correlations introduces larger bias in probabilistic constraints than incorrect distribution specification. Rabotyagov (2010) considered two agricultural conservation actions as well as spatial correlation for soil carbon sequestration. However, the introduction of multiple dimensions as well as distributional assumptions needed to make probability statements further complicate the issue. For instance, Kampas and Adamidis (2005) pointed out that under log-normality assumption of pollution reduction from a single action, the sum of reductions does not follow the log-normal distribution as Gren, Destouni, and Tempone (2002) assumed.

When, in addition, the natural science knowledge suggests that important dimensions of $S(\boldsymbol{x};\boldsymbol{\varepsilon})$ are nonlinear and nonseparable (e.g., examples provided in Carpenter et al. 2015), obtaining analytical expressions for the overall resilience value becomes much more difficult.

253 However, as in simulation-aided econometric estimation, simulation approximation to the
254 probability or other expected functions of interest such as the mean or the variance remains
255 available. One issue that arises in this context is computational cost associated with evaluating
256 $S(\boldsymbol{x};\boldsymbol{\varepsilon})$ many times. For example, we could build the objective of resilience directly into the
257 multiobjective tradeoff analysis (see Rabotyagov, Jha, and Campbell 2010) but instead we
258 choose to opt to formulate the objectives in terms of means and standard deviations. Resilience
259 is a property associated with a particular choice of actions to affect the provision of a vector of
260 desirable outputs. Basic theory and empirical work to date suggest that resilience is costly.
261 Resilience of the type we study is closely related to the variance in the desired output. To explore
262 the potential tradeoffs among cost and proxies for aquatic ecosystem services, as well as evaluate
263 potential synergies or tradeoffs associated with resilience, we choose to simultaneously optimize
264 for the cost of economic inputs, and the mean and the variance of non-market ecosystem outputs.
265 Further, we use bootstrap methods for a computationally fast way to provide resilience
266 assessment of the optimized solutions.

267 **Tradeoff Development**

268 An efficient tradeoff frontier in the production of ecosystem services emerges when all
269 Pareto-improvements have been exhausted: no single objective can be improved upon without
270 sacrifice in terms of other objective(s). Some of the objectives may be formulated as resilience
271 objectives. The classic example is tracing out the efficient mean-variance frontier of a stock
272 portfolio. For multiple objectives when the economic-ecological production function can be
273 explicitly written exact multiobjective optimization can generate tradeoffs across different
274 ecosystem services (see Polasky et al. (2008) and Toth and McDill (2009)). In the case that

$S(\boldsymbol{x};\boldsymbol{\varepsilon})$ function is cannot be written in a compact mathematical form but is represented by a computer simulation program, simulation-optimization methods can be used.

Multiobjective evolutionary algorithms are capable of dealing with potential non-convexities in optimization and can use simulation model output to (approximately) develop multiple-objective Pareto-efficient sets in a single optimization run. Deb (2001) is the classic introduction to evolutionary algorithms. Nicklow et al. (2010) and Maier et al. (2015) discuss some recent applications focused on water resources, and Kennedy et al (2008) and Porto et al (2014) provide terrestrial ecosystem management examples. Herman et al. (2014) explore tradeoff generation under deep uncertainty. Recent examples for tradeoff development using multiobjective evolutionary algorithms in agriculturally dominated ecosystems include Gramig et al. (2013), Bostian et al. (2015), Ahmadi et al. (2013), Rabotyagov et al. (2014) and Chichakly et al. (2013) who incorporate measures of resilience to anticipated climate change.

We consider a model of joint economic-ecological production process, where the human actions considered are "working land" agricultural conservation practices largely consistent with the prevailing crop system and "land retirement" of establishing perennial grass cover on cropland. These actions represent economic inputs into the production of (proxies for) freshwater and coastal aquatic ecosystem services associated with reducing nutrient fluxes, namely ambient Nitrogen (N) and Phosphorus (P) loads.

Scientific consensus exists on the fact that human activity has altered both the nitrogen and phosphorus cycles (Millenium Ecosystem Assessment, 2005, Ch. 12), with some beneficial (increased crop production), and some deleterious (eutrophication) effects on ecosystem services. The exact targets for nutrient loads and concentrations are an active area of research and policymaking (Evans-White et al., (2013), Heiskary and Bouchard (2015), US EPA, 2015 http://cfpub.epa.gov/wqsits/nnc-development/) but it is well understood that excess nutrient

299 loads negatively impact many ecosystem services from freshwater systems. We take as a starting
300 point that it is desirable to reduce N and P and elucidate the tradeoffs involved in controlling the
301 mean and standard deviation of nutrient pollution.

302 **Conceptual Model**

303 Our notation is similar to the notation used by Rabotyagov, Valcu, and Kling (2014).
304 There are K decision-making units ("fields") in the watershed, each field being characterized by
305 a unique combination of physical characteristics (soil, slope) and location in the watershed. The
306 ambient water quality is monitored both in stream and at the outlet of the watershed. Let $r_i =$
307 $r_i(\mathbf{x_i}, \xi)\ \forall\ i = 1, \ldots, K$ be the i^{th} field emissions given the actions taken at field level, where $\mathbf{x}_i$
308 represents the $J \times 1$ vector of actions implemented at each field, and ξ represents the stochastic
309 weather factor. The set of actions consists of baseline activity and a set of working land
310 conservation practices and land retirement.

311 To connect farm-level conservation actions to outcomes of interest, we need a specific
312 version of the ecological production function. In our application, this function is represented by a
313 water quality production function, $\mathrm{W}(\mathbf{r}(\mathbf{x}, \boldsymbol{\xi}))$ that is the result of the complex spatial interactions
314 between the edge-of-field emissions leaving the fields, and which is represented by an
315 ecohydrologic simulation model.[8] Given the stochastic nature of the weather factor, we are
316 interested in finding the least-cost spatial combinations **x** that reduce expected values of nutrient
317 pollution as well as its standard deviation. Using optimization results, we construct a measure of

[8] As Lichtenberg (2002) explains: "… there is not a simple monotonic relationship between emissions at the level of an individual field and impacts on environmental quality at the ambient scale with which policy is actually concerned. Fate and transport are typically non-linear and depend on space and time in complex ways, making extrapolation of field-level emissions to ambient pollutant concentrations quite complex". We refer the reader to Lichtenberg (2013), Shortle and Horan (2013) for reviews of these and other issues associated with nonpoint source pollution from agriculture, as well as to Rabotyagov et al (2014) for an attempt to simplify the 'ecological production' process. Uncertainty in the model structure itself is not considered in this article, although we recognize this as likely important for both better science and policy-relevance (see Herman et al. 2014).

318 resilience defined as the probability of achieving a particular target, and analyze the tradeoff
319 between costs and different levels of resilience. We start by considering the case of a single
320 nutrient pollutant (a proxy for diminished aquatic ecosystem services upstream and downstream)
321 and then move to the case of two pollutants.

322 *A single pollutant case*

323 We begin by solving the multi-objective problem that simultaneously minimizes

324 $$Min_{\mathbf{x}}\left[\, C(\mathbf{x}),\ E_T[N(\mathbf{x})]\,, Var[N(\mathbf{x})]^{0.5}\right] \quad (1)$$

325 where $\mathbf{x}$ represents a $KJ \times 1$ vector representing a particular placement of conservation practices,
326 $\mathrm{W}\big(\mathbf{r}(\mathbf{x},\boldsymbol{\xi})\big) \equiv N(\mathbf{x})$ represents the simulated, over simulation period of length T, vector of
327 annual nitrogen loads, $E_T[N(\mathbf{x})]$ is the mean nitrogen loads over the historical simulation
328 period, $Var[N(\mathbf{x})]^{0.5}$ is the standard deviation, and $C(\mathbf{x})$ is the (deterministic) estimated cost of
329 that particular combinations of conservation investments (economic inputs into aquatic
330 ecosystem service production) in the watershed.

331 The solution vector $\mathbf{x}^*$ defines the Pareto-efficient set (P_f), where each element is
332 represented by a unique combination of cost, expected nutrient load and the standard deviation of
333 loads:

334 $$P_f(\mathbf{x}^*) = \left\{C(\mathbf{x}^*), E_T[N(\mathbf{x}^*)]\,, Var[N(\mathbf{x}^*)]^{0.5} \;\middle|\nexists\, \mathbf{x} \neq \mathbf{x}^*, P_f(\mathbf{x}) \succ P_f(\mathbf{x}^*)\right\} \quad (2)$$

335 That is, a pattern of conservation investments defines the Pareto-efficient frontier if there is no
336 other conservation action pattern which is a Pareto-improvement ($\succ$) in the cost-mean-standard
337 deviation space. The Pareto-efficient frontier defines the set of optimal tradeoffs; for example,
338 the lower envelope of the set with respect to mean N and conservation action costs gives the
339 equivalent of the total abatement cost curve for expected nutrient pollution. It also offers

valuable information on the possible mean-variance tradeoffs, where, for a given cost, a tradeoff between expected ecosystem service performance and its standard deviation could be seen. However, we cannot directly infer how much would it cost to achieve a particular level of nitrogen loads under different levels of resilience, where by resilience, we understand the probability of achieving that target in any given year. However, for the single stochastic objective, it is straightforward to "collapse" the three-dimensional Pareto-frontier into a set of "resilient tradeoffs" between cost and resilient provision of an ecosystem service. Doing so involves appropriately constructing the deterministic equivalent to the resilience objective using the mean, standard deviation, and the critical value of the controlled distribution of the stochastic objective.

Finding resilient solutions involves solving a chance- constrained optimization problem:

$$Min_{\mathbf{x}}\, C(\mathbf{x})\ \ s.t.\ \ \Pr\{\mathrm{N_t}(\mathbf{x}) \leq \overline{N}\} \geq \alpha \quad \forall t = 1, \dots, T \tag{3}$$

where $\overline{N}$ is the target level of N loads, and α the desired level of resilience measured as the probability of achieving the target.

We use the Pareto-frontier $P_f(\mathbf{x}^*)$ and employ two approaches to approximate solutions to the above problem, approaches that we identify as "normal" and "non-parametric". Under both approaches, we transform equation (3) using its deterministic counterpart as:

$$Min_{\mathbf{x}}\, C(\mathbf{x})\ s.t.\ \ E_T\{\mathrm{N}(\mathbf{x})\} + \phi^{\alpha} Var(N(\mathbf{x}))_T^{0.5} \leq \overline{N} \tag{4}$$

where ϕ^{α} is the critical value of the standardized distribution of $N(\mathbf{x})$.

Note that a solution to the chance-constrained problem (3) must be a member of the Pareto frontier in the cost-mean-standard deviation space: $\hat{\mathbf{x}} \subset \mathbf{x}^*$. The converse is not true: that is, a particular solution from a multiobjective optimization program need not be optimal for a

chance-constraint program. Appendix 1 in supplemental materials provides the demonstration of this point.

Under the normal approach, we assume the standardized distribution of pollution load follows a normal distribution and use $\phi^{\alpha} = \Phi^{-1}(\alpha)$, the standard normal critical value that depends on α (1.64 for $\alpha = 0.95$). Under the normality assumption, we consider $\alpha - resilient$ pollution loads to be $E_T\{\mathrm{N}(\hat{\mathbf{x}})\} + \Phi^{-1}(\alpha)Var(N(\hat{\mathbf{x}}))_T^{0.5}$ and can focus on the results in terms of tradeoffs between cost and resilient nitrogen loads.

Non-parametric approach

An alternative approach is to employ non-parametric bootstrap methods (Efron (1979)), and define the resilience pollution loads in terms of the bootstrapped quantiles. Since our data (nitrogen loads simulated over a period of time) is serially dependent, we employ the block stationary bootstrap method (Politis and Romano (1992), (1994)). Under this approach, observations are re-sampled in blocks of random length, with the length of the block being determined by a geometric distribution. The block re-sampling (observations are drawn consecutively) preserves the lag dependence in the original data. The bootstrapped data is stationary if the block length is determined using a geometric distribution. Additionally, the block bootstrap works well under very weak conditions on the dependency structure of the original data.

For any efficient combination of conservation practices ($\mathbf{x}^*$) that is part of the Pareto frontier $P_f(\mathbf{x}^*)$, we take the model-simulated $T \times 1$ vector of nitrogen values $N(\mathbf{x}^*)$ to construct a non-parametric distribution using a stationary bootstrapping approach using blocks of unequal length. To obtain tradeoffs involving $\alpha - resilient$ nitrogen loads, we compute, for each bootstrap replicate series, the sample α-quantile and average the results over many bootstrap

replications. The interpretation of the new $\alpha - resilient$ Pareto frontier is similar to the previous one, each solution representing a non-dominated combination of cost and $\alpha - resilient$ nitrogen loads that correspond to a given level of resilience, α. The magnitude of the differences between the normal and non-parametric approaches is an empirical question.

Multiple pollutants: A case of nitrogen and phosphorus

We also consider developing tradeoffs which involve the means and the variances of multiple ecological objectives. In this case, we modify the multiobjective minimization problem to include the means and standard deviations of two nutrient pollutants, nitrogen and phosphorus:[9]

$$Min_{\mathbf{x}}\,[\,C(\mathbf{x}),\ E_T[N(\mathbf{x})]\,, Var[N(\mathbf{x})]^{0.5}, E_T[P(\mathbf{x})]\,, Var[P(\mathbf{x})]^{0.5}] \quad (5)$$

where $\mathbf{x}$ represents a particular placement of conservation practices, $N(\mathbf{x})$, $P(\mathbf{x})$, the vectors of nitrogen and phosphorus loads of length T, $E[.]$ is the expected water quality outcome measured as (historical) sample mean of nitrogen and phosphorus, $Var[N(\mathbf{x})]^{0.5}$ and $Var[P(\mathbf{x})]^{0.5}$ are respective standard deviations, and $C(\mathbf{x})$is the estimated annual cost of the particular combination of conservation investments in the watershed.

Similarly to the univariate case, the solution is represented by a Pareto set, P_f^{NP}, where each element represent a non-dominant combination of cost, mean and standard deviation values for nitrogen and phosphorus emissions associated with a spatial combination of conservation practices. As discussed above, it is more intuitive to consider actual tradeoffs between mean and

[9] If the objective were to be specified as minimizing the variance, for example, the sum, or a linear index of two nutrients, the covariance term would enter into problem specification. Alternatively, the resilience objective specified as a joint probability could be simulated within the optimization loop (as in Poojari and Varghese (2008)). We leave those extensions to future work.

404 variance control or to characterize a particular solution in terms of a probability (resilience value)
405 of meeting a specified target.

406 In order to characterize joint resilience implied by the solutions in the Pareto-frontier, we
407 rely on the nonparametric bootstrap, now using two dimensions. Resilience is defined as the joint
408 simulated probability of achieving both N and P targets. Similarly to the univariate stationary
409 bootstrapping, we use the vectors of simulated nitrogen and phosphorus loads to generate
410 bootstrap replicates using blocks of unequal length. The stationary bootstrapping procedure
411 involves using both vectors simultaneously, thus preserving the correlation between controlled
412 loads of N and P. That is, given a particular joint target ($\bar{N}, \bar{P}$), we can construct characterize the
413 tradeoff frontier in terms of cost, mean nitrogen, mean phosphorus and simulated joint resilience
414 of achieving the specified target. The resilience level is estimated as the simulated probability,
415 $p(\mathbf{x_i})$:

416 $$p(\mathbf{x_i}) = \sum_{r=1}^{M}\{\sum_{t=1}^{T} I(N(\mathbf{x})_{rt} \leq \bar{N}\,, P(\mathbf{x})_{rt} \leq \bar{P})/T\}/M \quad (6)$$

417 where T is the length of the model simulation, $\mathbf{x_i}$ is the particular pattern of conservation
418 investments evaluated and M is the number of bootstrap repetitions.

419 To approximate the solution sets for the multiobjective problems (1) and (5), we use a
420 simulation-optimization framework using Soil and Water Assessment Tool (SWAT) as the
421 simulation model and a modification of the Strength Pareto Evolutionary Algorithm 2 (SPEA2)
422 (Zitzler, Laumans, and Thiele, 2002) as the multiobjective optimization heuristic, as described by
423 Rabotyagov et al. (2010). The simulation-optimization framework simultaneously minimizes the
424 cost, the 20-year means ($T = 20$) and standard deviations of annual N for the single pollutant

425 case and N and P loads for the two pollutant case.[10] The solutions are sets of Pareto-
426 nondominated watershed configurations P_f and P_f^{NP}. To assess convergence, we use a
427 consolidation ratio proposed by Goel and Stander (2010) and used by Rabotyagov et al. (2014).

428 SWAT is designed to run watershed simulations based on a wide range of inputs: weather
429 data, soil characteristic, plant growth and crop rotations, nutrient management, nutrient transport
430 and transformation, land use and management practices. The model can be used to estimate the
431 changes in nutrient emission in response to the land changes associated with alternative
432 conservation practice, crop choices, and rotation alternatives. The model was developed by the
433 U.S Department of Agriculture and has been used in a wide range of applications (Arnold et al.
434 (1998); Arnold and Fohrer (2005); and Gassman et al. (2008)).
435

436 **Empirical Application: The Boone River Watershed**

437 Our empirical results focus on The Boone River Watershed (BRW). The BRW is a
438 typical agricultural watershed in central Iowa with more than 90% of its area dedicated to corn
439 and soybean production. The watershed's tributaries offer habitat to the Topeka shiner, a
440 federally listed endangered species, and to other fish and mussel species. Additionally, the
441 watershed tributaries feed the Des Moines River, a major water source for the biggest
442 metropolitan area in Iowa. The lower part of the watershed is used for recreation activities.
443 Given the extent of the agricultural activities, high levels of agriculture-contributed
444 nitrogen, phosphorus and sediment loads contribute to the water quality impairments. A

[10] The resulting relatively small sample size used to construct the model-simulated mean and the standard deviation is one of the limitations of the study, and can introduce imprecision in resilience estimates. To the extent that mean and standard deviation estimates are not biased, we try to improve precision by bootstrapping optimized series.

successful calibration for the current Boone River Watershed SWAT baseline was obtained by using monthly streamflow nutrient data and incorporating earlier calibration efforts (Gassman, (2008)).[11] The set of conservation practices selected for achieving the nutrient reduction includes working land practices: cover crop, no-till, the combination of cover crops and no-till, and land retirement. Typically, cover crops are grown during late fall and early spring. In the Midwest, where there are no markets for cover crops, cover crops are promoted for their direct environmental benefits (recycle nutrient and prevent nutrients leaching) and indirect economic benefits (improve soil health by preventing soil erosion). Cover crops are effective in reducing both nitrogen and phosphorus losses. No-till is a type of tillage where no more than 30% of the crop residue is removed. No-till is effective in reducing erosion and phosphorus runoff. Land retirement involves taking land out of production and the establishment of perennial grasses.

The costs estimates for conservation practices used in this study are drawn from several sources: no-till at $6 per acre (Iowa State Extension budgets), cover crops at $35 per acre (Iowa Nutrient Reduction Strategy), $41 per acre for the combination of no-till and cover crops, and $254 per acre, the average cash rental rate for the BRW (Iowa State Extension cash rental rates estimates) as the cost of land retirement. The cost of conservation practices is additional to the cost of baseline activities, considered to be zero in this application.

Results and discussion

The simulation framework allows us to evaluate counterfactual watershed-based scenarios in terms of estimated costs of conservation practices and their implications for mean

[11] The present SWAT simulations are being performed with an updated SWAT version 2012 code (SWAT2012, Release 6150 that contains corrected algorithms that more correctly simulate movement of nitrate through subsurface tile lines as well as numerous other enhancements that were not present in the SWAT2005 code.

and variance of corresponding nutrient loads over a 20-year period (1993-2013). We estimate the Pareto- efficient frontiers for a single pollutant (N) and multiple pollutants (N and P). We offer a short analysis of the mean-variance tradeoffs and how these tradeoffs relate to the choice of the conservation actions. Next, we analyze the trade-offs between achieving a pollution target with a given resilience level and the estimated cost of conservation actions. The set of resilience values (α) ranges from 50 percent to 95 percent in increments of 5 percent, as well as 99 percent. Nutrient pollution targets are chosen to be equivalent to a range of percent reductions from the historical baseline emissions.

Single pollutant case: Nitrogen, Mean-Variance Tradeoffs

The results of the multi-objective optimization defined by equation (1) can be visually depicted by a three dimensional scatterplot (P_f), where each point on the frontier represents the least cost watershed configuration that achieves a given expected value of N loads and has the lowest standard deviation (see Figure A2 in the supplementary material). Figure 1 depicts the extent of the mean-variance tradeoffs from the frontier. Specifically 1(a) shows a fairly linear positive relationship between the mean and the standard deviation of N loads, as standard deviations increase with the means. Additionally, the analysis of mean-coefficient of variation (ratio of standard deviation to the mean) plot (Figure 1(b)) shows three patterns: a steep increasing trend for the low range nitrogen emissions (below three thousand tons) where the standard deviation increases at a faster rate than the mean, followed by a smoother declining pattern where the standard deviation increases at a slower rate than the mean. For larger loads (above 4.5 thousand tons), the ratio of standard deviation to mean settles around 0.5. These patterns can be explained by the distribution of the conservation practices selected by the algorithm (see supplementary material Figure A3).

Next, we quantify the cost to achieve a particular level of nitrogen loads under different levels of resilience. More explicitly, for any level of resilience α, we construct resilient Pareto frontiers, where each Pareto frontier can be viewed as the total cost curve where the corresponding nitrogen emissions are achieved with probability α. As previously described, we use two approaches (normal and non-parametric) to construct the resilient Pareto frontiers that corresponds to different resilience levels. The "normal" approach assumes that the standard normal critical values are used to weigh the standard deviations, while the non-parametric approach uses stationary bootstrap to simulate the quantiles. Simulated nutrient load series pass stationarity tests, and we use 10,000 bootstrap replications with mean block length of 5. The new Pareto frontiers transform the mean nitrogen values of the original Pareto frontier into α resilient levels while keeping the costs and the watershed configurations unchanged.

Figures 2 depicts the α resilient Pareto frontiers for four levels of resilience: median (50), 75, 90, and 99 given the two approaches, as well as the mean-cost tradeoff. The horizontal axis depicts the resilient loads, and the vertical axis shows annual costs. Notice that under the normal approach (left panel), the corresponding levels of resilience for mean and median are identical, while under the non-parametric approach the two tradeoff frontiers are different, the bootstrapped mean curve being entirely above the median (right panel). Under the both approaches, the Pareto frontiers move further away from the left corner as the resilience levels increase. For any cost level (consider a horizontal line), the resilient level of N loads increases as we move from one frontier to another. This shows us how much resilience can be achieved under a given budget. Likewise, for any level of resilient N loads, the cost increases as we move from one frontier to another. The distance between two consecutive frontiers represents how much it would cost to make the same level of N load more resilient. (Pairwise comparisons between the two distributions are provided in the supplementary material).

512 Each cost-resilient curve corresponds to a resilient N target expressed as a percentage
513 reduction from the baseline. As expected, more stringent targets (higher percentage reductions,
514 lower loads) cost more and the costs of achieving a given target increases with the resilience
515 level. For less stringent targets, the costs-resilience curves are convex, with a non-convexity
516 patterns for more stringent targets. For example, when the target is set to 70 percent reductions,
517 the cost is flat once a high level of resilience (80) is achieved.

518 *Resilience-Marginal Cost Curves*

519 Another way to analyze the resilience-cost trade-off is to answer the question how much would it
520 cost to achieve an additional level of resilience. We focus our analysis on three levels of
521 reductions: low (20 percent), average (the Iowa Nutrient Reduction Strategy 45 percent), and
522 high (70 percent reductions). For each of the three targets, Figure 3 summarizes the cost curves
523 for securing the targets at an additional resilience level. These curves can be interpreted as the
524 marginal cost of resilience. Although the marginal cost curves have a similar shape, their
525 magnitudes differ across the two approaches. The marginal cost curve when the target is low (20
526 percent reductions) is almost flat for resilience levels lower than 80. However, for higher
527 resilience, the marginal costs display a sharp increase, with the increase being sharper under
528 normal approach. The marginal cost curve for the intermediate target displays more than one
529 pattern. Under the normal approach, marginal costs are increasing for lower resilience, linear for
530 moderate resilience, and again increasing for higher resilience levels. However, the patterns are
531 different under the non-parametric approach: linear for lower levels, increasing for moderate
532 levels, decreasing and linear for higher levels of resilience. The marginal costs for the most
533 stringent target are increasing for lower levels, decreasing for moderate levels, and linear for
534 higher resilience level. The diversity of patterns across targets and resilience levels can be

explained by the distribution of the conservation practices (these are provided in Table A1 of supplementary materials). The costs of achieving resilient loads corresponding to 45 percent reductions (3.39 thousand tons) range from 13 to 87 million over the considered resilience levels. Similarly to McSweeny and Shortle (1990), we find that to control a single-year N load with 99 percent resilience is almost 7 times costlier than controlling N with median resilience

Resilient N loads for different cost (budget) levels

The α resilient Pareto frontiers can also provide insight into the different load levels that can be secured under different levels of resilience when we impose a limit on total costs (iso-cost curves). Figure 4 can be used to see how much resilience can be obtained under a given budget. Next, we present the results for four cost (budget) levels: 10, 20, 50, and 100 million. For each budget level, we construct iso-cost curves showing the tradeoffs between resilience and different levels of attainable loads.

Figure 4 shows that the iso-costs are convex shaped, showing that when considering cost constant, higher levels of resilience translate in higher levels of emissions, or alternatively lower emission level have lower resilience levels. The empirical findings also show that the size of these tradeoffs decrease as the total costs increase, as the iso-cost curves corresponding to lower total cost have steeper slopes. For any of the chosen cost and any resilience levels, fewer emissions (more reductions) can be claimed under the non-parametric approach (Figure 4 right vs. left panel). Also, the slopes of the non-parametric iso-cost curves are smoother.

Multiple targets: nitrogen and phosphorus

Next, we present the simulation results for the case when two pollutants (N and P) are jointly targeted. We approximate the Pareto-frontier for 5 objectives: cost and means and standard

557 deviations of N and P. Pareto-frontier we obtain is valuable in that can show the nature of
558 tradeoffs along different values of N and P as well as corresponding variability and cost.

559 Visualizing tradeoffs across more than two dimensions is challenging, and pairwise
560 projections of the Pareto-frontier could be most helpful to see a particular scope of synergies or
561 tradeoffs. Visualizing across 5 dimensions is possible; however, interpretation can be
562 challenging. To aid this process, we present a radar (spider) plot in all 5 dimensions. Specific
563 solutions of interest (a few at a time) can be analyzed as well. Consider the left panel of Figure
564 5, and the mean N (mean P) and Cost axes. The non-convex shape of the plot between those axes
565 says that there are no solutions in the Pareto-frontier which simultaneously have high cost and
566 high mean N (and P) loads (and compensating for those with smaller values on other axes). This
567 suggests a strong tradeoff existing between mean nutrient loads and cost. A convex shape with
568 respect to other axes *does not* mean that tradeoffs do not exist among the remaining pairs of
569 objectives, but that there *exist* efficient solutions which exhibit synergies (co-movement) along
570 those dimensions. For example, as we see subsequently (Figure 6), tradeoffs between N and P
571 control exist, but synergies are also present (pairwise comparison of mean N and P on the right
572 panel of figure 5). A presence of at least some synergies is also apparent by considering pairwise
573 tradeoffs between means and standard deviations (consistent with a limited nature of mean-
574 variance tradeoff for N explored above). Whereas, as can be seen from the nature of the tradeoffs
575 between costs and standard deviations (shown on the right panel of Figure 5 for the case of
576 standard deviation of P—N results are similar), there are no synergies between cost and risk, and
577 we see strong tradeoffs consistent with the notion that resilience is always costly. However, we
578 do not see strong tradeoffs between means or standard deviations of nutrient reduction
579 objectives. Of course, this finding may not generalize to other contexts.

580 Next, we make the connection to resilience. Note that, unlike in a single stochastic
581 objective case, we can no longer claim that a solution to a chance-constrained formulation has to
582 be a member of the Pareto-frontier. For the case of separate resilience objectives, where each
583 pollutant has be controlled in a resilient fashion that is still the case (using the same logic as
584 above). That is, single pollutant resilient levels can be obtained in exactly the same way we
585 proceeded above with N. Because of that reason, we do not present single-pollutant resilience
586 tradeoffs.

587 However, if one is interested in the joint constraint of the type: $\Pr\{\mathrm{N_t}(\mathbf{x}) \leq \overline{N}, P_t(\mathbf{x}) \leq$
588 $\overline{P}\} \geq \alpha \quad \forall t = 1, \dots, T$, we cannot be assured of joint resilience optimality of solutions obtained
589 by the multiobjective program, as the algorithm does not directly simulate joint probability
590 which is a function of variances and the covariance between N and P. To assume cost-joint
591 resilience efficiency for specific $\overline{N}$ and $\overline{P}$ targets, one could formulate a two-objective
592 evolutionary optimization program involving cost and simulated probability of joint goal
593 attainment (akin to Poojari and Varghese (2008) or Rabotyagov, Jha, and Campbell (2010)).
594 Despite the possibility that the solutions in the Pareto frontier may not be optimally resilient for
595 joint nutrient targets, we can still provide ex-post assessment of the solutions in terms of joint
596 resilience. To do so, we again rely on (now joint) non-parametric bootstrap approach, using
597 10,000 replicates and computing the simulated resilience using (6).

598 A three dimension illustration of these tradeoffs when the targets are set equal to 45
599 percent reductions for both N and P (equation 9) is presented in the supplemental material
600 (Figure A6). Each element on this frontier (a 3-dimensional projection of the 5-dimensional
601 Pareto-frontier P_f^{NP}) is assessed for a resilience (probability) level of achieving this joint target.
602 As for the single pollutant case: securing higher level of resilience demands higher costs. We

present the lower envelopes of the plot in Figure 6. Figure 7 depicts the marginal costs of achieving additional levels of resilience for the three specified targets, while Table A2 (contained in supplementary details) describes in detail the total and marginal costs as well as the distribution of conservation practices. For example, the least cost way to achieve 45 percent reductions with 70 percent resilience is higher than the least cost to achieve the same level of reductions with 75 percent resilience (Figure 6). The negative marginal costs are unexpected but we interpret them as the inefficiencies embedded in the spikes, and, should one focus on a specific set of N and P reductions with a resilience objective, we expect those to disappear. With those caveats in mind, we provide a broad assessment of joint resilience implied by the 5-dimensional Pareto-frontier.

Overall, the costs of achieving the joint target are higher than in the case of a single pollutant and range from 22.3 to 107.4 million. This is to be expected as a joint probability is going to be smaller than a marginal one. The distribution of the conservation practice is different, with more land retirement being used more extensively at any resilience level. The spatial placement of the conservation practices associated with these solutions is provided in the supplemental materials.

Conclusions and caveats

Many ecosystem services are rival and important tradeoffs exist in their production process. Understanding the nature of these tradeoffs requires: *(a)*defining a quantifiable measure of the underlying ecosystem production process and of the economic inputs that go into this productions functions, and *(b)* exploring alternative resource allocation decisions to identify, if only approximately, Pareto-efficient ways of producing different ecosystem services. Uncertainty in the provision of a particular ecosystem service adds another dimension to the

626 nature of these tradeoffs, where different ecosystem services differ both in terms of the expected
627 outcomes and in terms of risks. Closely related to uncertainty is the notion of resilience, and the
628 cost of providing the ecosystem service under different levels of desired resilience.

629 We focus on understanding and quantifying the tradeoffs for the case of proxies for
630 aquatic ecosystem services in the landscapes dominated by agricultural activity. Particularly, we
631 focus on controlling the flux of agricultural nutrients (N and P) as means to improve the
632 upstream and downstream water quality. Economic inputs into water quality production are a set
633 of conservation practices that can be implemented on agricultural landscapes for controlling the
634 flux of nutrients, while the (intermediate) ecological production function is an ecohydrologic
635 simulation model relating human actions to changes in nutrient loads. By integrating a heuristic
636 global optimization with a ecohydrologic model we meet the conditions of having science-based
637 representation of the water quality production function ($W_t(\mathbf{r}(\mathbf{x}, \boldsymbol{\xi}_t))$) and its dependence on the
638 exogenous stochastic weather factors and of having the ability to produce an approximate Pareto-
639 frontier that accounts for multiple tradeoff dimensions.

640 We quantify the tradeoffs involved in achieving different levels of nutrient loads with
641 different levels of resilience where resilience is defined as the probability of attaining the desired
642 level of nutrient load. We spatially optimize the selection of least-cost patterns of agricultural
643 conservation practices or both the expected performance of the conservation actions and its
644 variance. We analyze the tradeoffs for a single nutrient (ecosystem service), and then expand our
645 analysis to include multiple nutrients (multiple ecosystem services).

646 We apply our modeling framework to the Boone River Watershed in Iowa. The empirical
647 results confirm expectations and are consistent with previous studies: securing nutrient loads
648 with higher level of resilience is costly. However, the marginal cost is not necessarily increasing:

649 that is, focusing on larger nutrient reductions allows one to obtain resilience at a smaller
650 additional cost than if one is seeking only modest nutrient reductions. In our application, this is
651 due to the ability of perennial grassland to buffer against exogenous shocks and to drastically
652 reduce variability in nutrient loads (as shown before, e.g., in Rabotyagov, Jha, and Campbell
653 2010). Furthermore, the main tradeoff dimension is between cost of conservation investments
654 and ecosystem service objectives, as opposed to pronounced mean-variance tradeoffs or strong
655 tradeoffs between the two nutrient objectives. While some meaningful tradeoffs exist between
656 nutrient objectives, our findings highlight the presence of relative synergies in agricultural
657 conservation investments aimed at nutrient reductions. However, while *relative* synergies exist,
658 controlling risk of nutrient loads has high opportunity costs, and resilience comes at a significant
659 premium.[12]

660 Among many caveats, we point out that our optimization algorithm was not exactly
661 tailored to the optimal joint resilience question, but instead focused on providing an overall
662 picture of feasible tradeoffs. Additional limitations associated with uncertainty in model
663 structure, the simplicity of economic cost representation, and the level of spatial resolution of the
664 ecohydrologic model present ample opportunities for future research. However, we hope to show
665 the utility and the promise of the general approach which integrates scientific understanding of
666 complex systems with the practical need to see how production of non-market ecosystem
667 services can be accomplished at the lowest possible sacrifice of economic inputs.

668

[12] We note recent research by Carpenter et al. (2015) who provide examples where, in nonlinear systems, reducing high-frequency variance can lead to an increase in low-frequency variance, thereby undermining the resilience objective. We constructed spectrum plots of controlled variance of nutrients and we see a decrease in variance at all spectra with an increase in conservation investment cost.

669

670

671

672 Figure 1 (a) Mean-Variance Trade-Offs (b) Mean-Coefficient of Variation

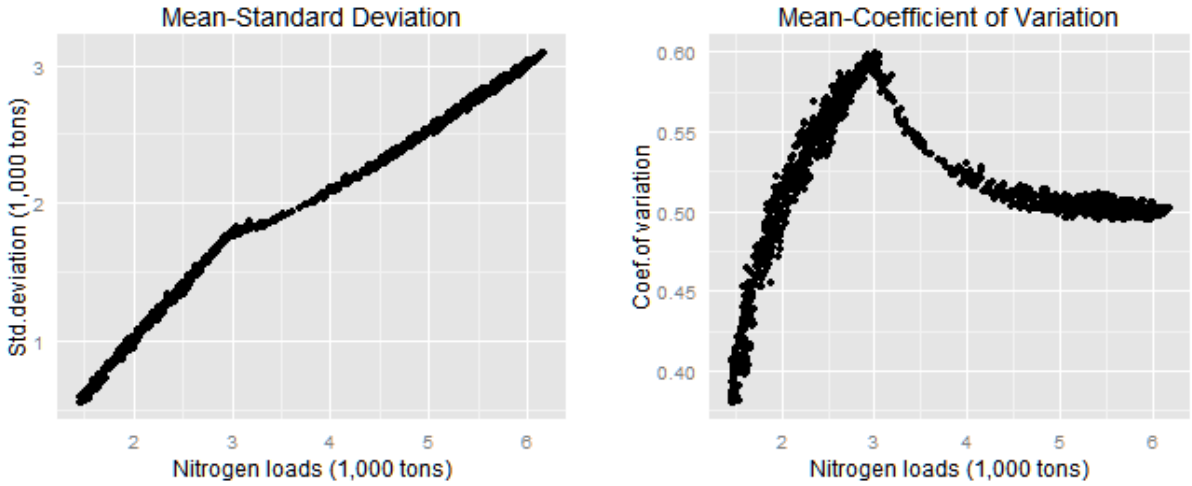

673

674

675

Figure 2: α Resilient Pareto Frontiers (Normal Approach (left), Non-parametric Approach (right))

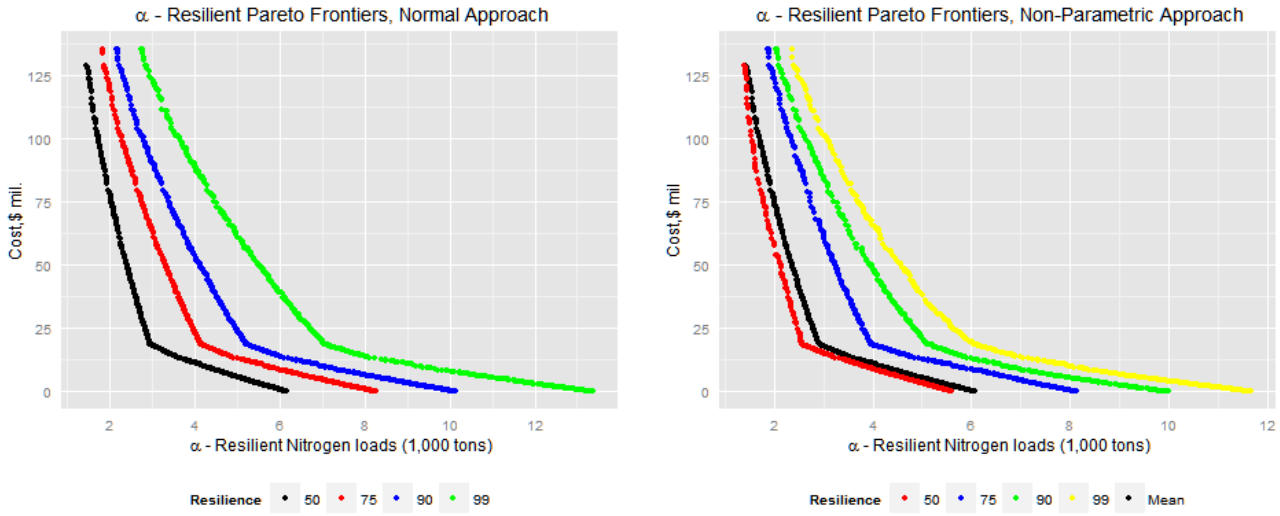

Figure 3 Marginal Costs of Additional Resilience for Different Resilient N Targets

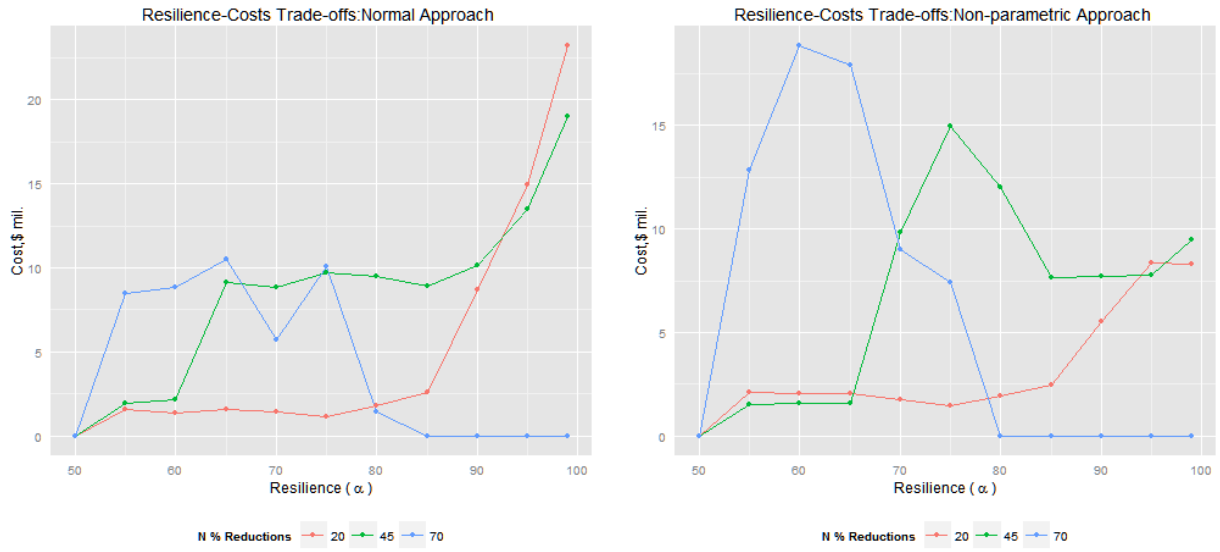

693 Figure 4 Resilience: Iso-Cost Curves(Normal Approach: left, Non parametric approach right)

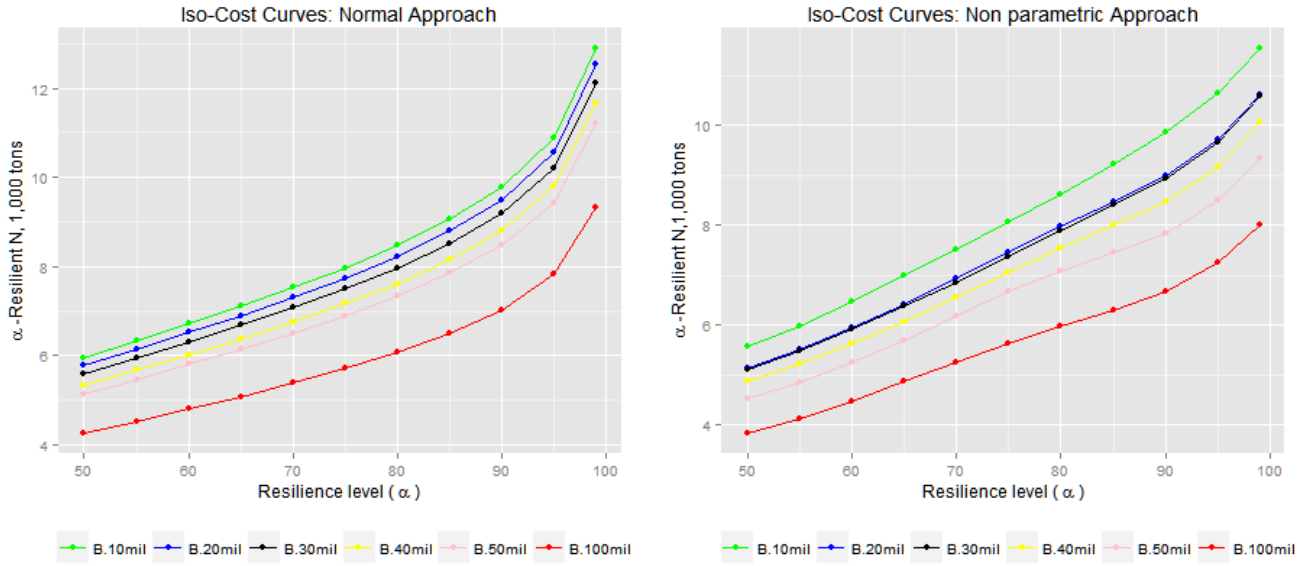

694

695

696

697

698

699

700

701

702

703

704

Figure 5. Pareto Optimal Frontier: Cost, Means (N, P), Standard deviation (N ,P)

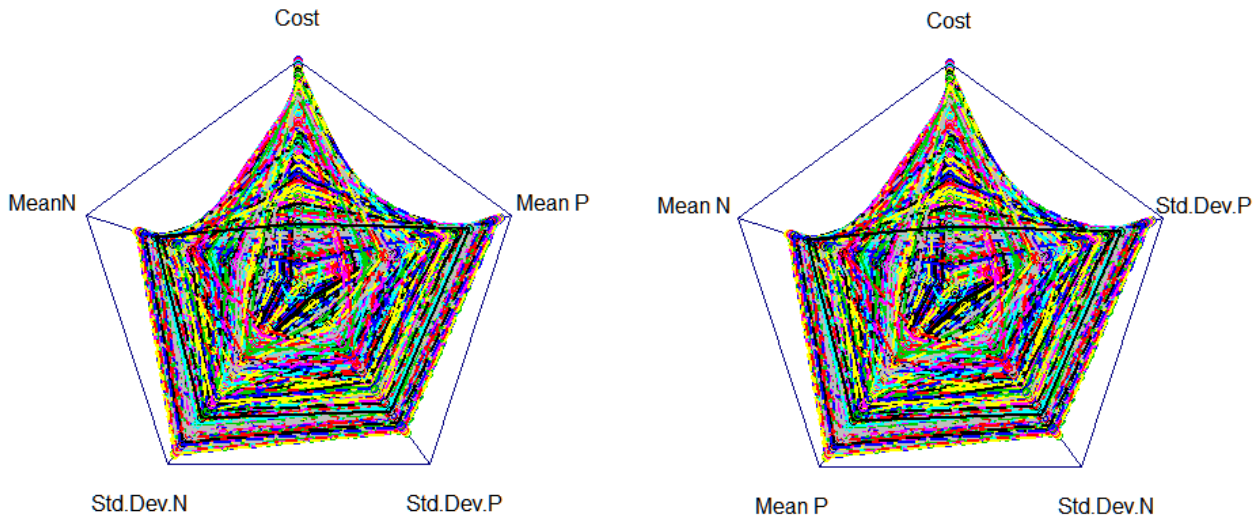

Figure 6 Cost of Achieving Resilience When Target is Equal to 45 percent Reductions for Both N and P.

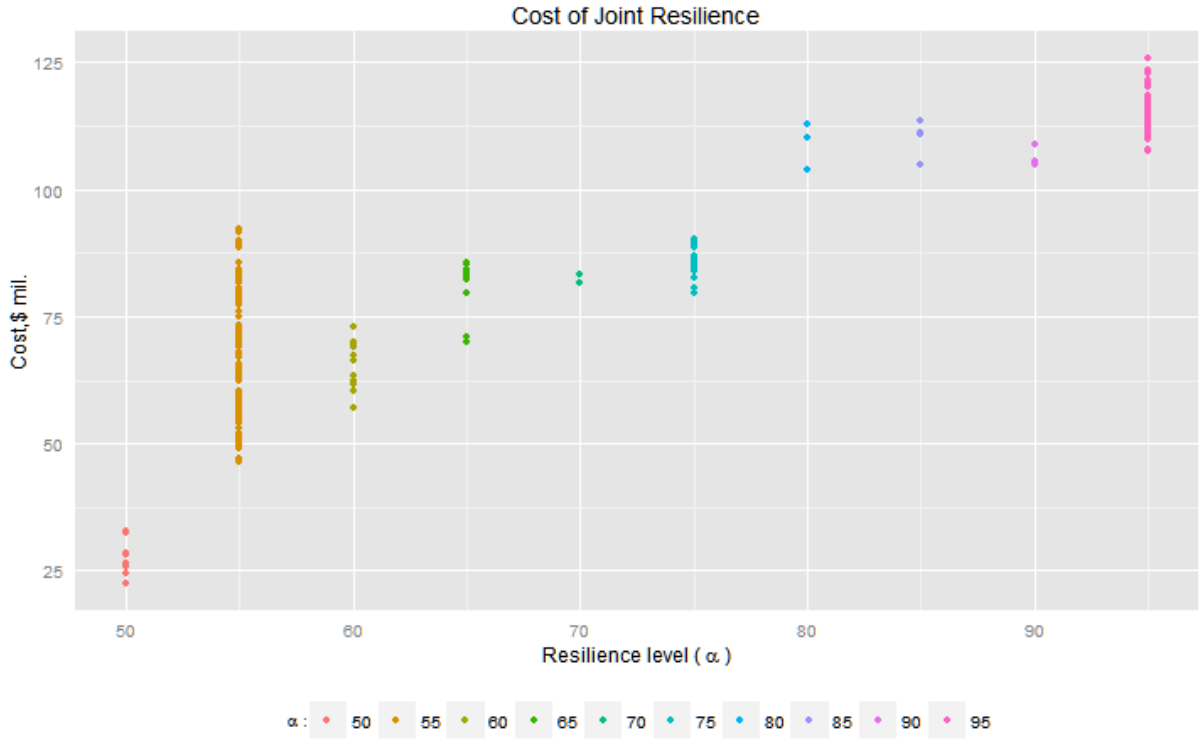

729 Figure 7 Marginal Costs of Joint Resilience

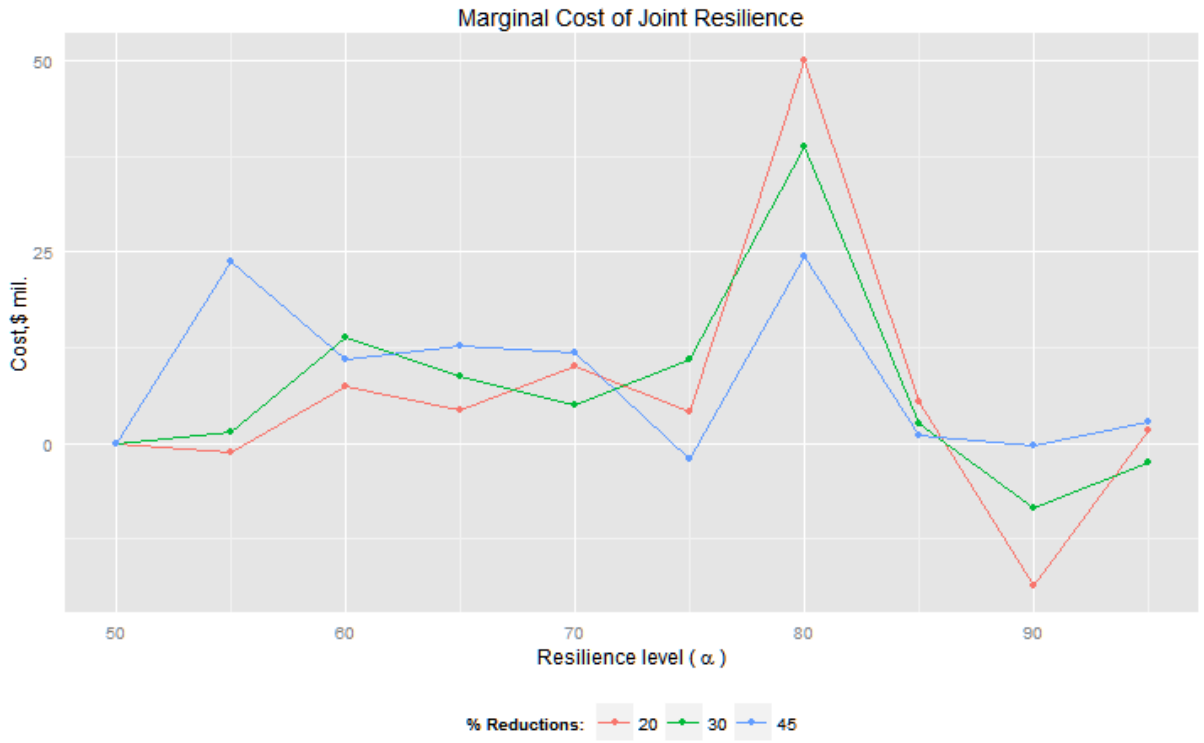

730

731

732

733

734

735

736

737 **References**

738 Ahmadi, M., Arabi, M., Hoag, D. L., & Engel, B. A. 2013. A Mixed Discrete-Continuous
739 Variable Multiobjective Genetic Algorithm for Targeted Implementation of Nonpoint Source
740 Pollution Control Practices. *Water Resources Research* 49(12): 8344-8356.

741 Arnold,J.G.,R.Srinivasan, R.S., Muttiah, and J.R.Williams.1998.Largeareahydrologic modeling
742 and assessment part I: model development. *Journal of the American Water Resources*
743 *Association* 34(1): 73–89.

744 Arnold, J. G. and N. Fohrer. 2005. SWAT2000: current capabilities and research opportunities in
745 applied watershed modelling. *Hydrological processes*, *19*(3), 563-572.

746 Barbier, E. B., Koch, E. W., Silliman, B. R., Hacker, S. D., Wolanski, E., Primavera, J., ... &
747 Reed, D. J. 2008. Coastal Ecosystem-Based Management with Nonlinear Ecological Functions
748 and Values. S*cience* 319(861): 321-323.

749 Bateman, I., A. R. Harwood, G. M. Mace, R.T. Watson, D.J. Abson, B.Andrews, A. Binner et al.
750 2013."Bringing Ecosystem Services into Economic Decision-making: Land Use in the United
751 Kingdom." *Science* 341(6141): 45-50.

752 Bawa, V. S. 1973. On Chance Constrained Programming Problems with Joint
753 Constraints. *Management Science 19*(11): 1326-1331.

754 Beavis, B., and M. Walker. 1983. Achieving Environmental Standards with Stochastic
755 Discharges. *Journal of Environmental Economics and Management 10*(2):103-111.

756 Bigman, D. 1996. Safety-first Criteria and their Measures of Risk. *American Journal of*
757 *Agricultural Economics 78*(1): 225-235.

758 Bostian, M., G. Whittaker, B. Barnhart, R. Färe, and S. Grosskopf. 2015. Valuing Water Quality
759 Tradeoffs at Different Spatial Scales: An Integrated Approach using Bilevel Optimization. *Water*
760 *Resources and Economics* 11:1-12.

761 Boyd J., and S. Banzhaf. 2007. What are Ecosystem Services? The Need for Standardized
762 Environmental Accounting Units. *Ecological Economics* 63(2-3):616–626.
763 Byström, O., H. Andersson, and M. Gren. 2000. Economic Criteria for using Wetlands as
764 Nitrogen Sinks under Uncertainty. *Ecological Economics*, *35*(1): 35-45.
765 Carpenter, S., R., Brock, W. A., Folke, C., van Nes, E. H., and M. Scheffer. 2015. Allowing
766 Variance May Enlarge the Safe Operating Space for Exploited Ecosystems. *Proceedings of the*
767 *National Academy of Sciences* (11): 800-804.
768 Charnes, A., and W.W. Cooper, W. W.1959. Chance-constrained programming. *Management*
769 *science*, *6*(1), 73-79.
770 Cherubini, U., E. Luciano, and W.Vecchiato. 2004. *Copula Methods in Finance*. John Wiley &
771 Sons.
772 Chichakly, K. J., W.B. Bowden, and M.J. Eppstein. 2013. Minimization of Cost, Sediment Load,
773 and Sensitivity to Climate Change in a Watershed Management Application. *Environmental*
774 *Modelling & Software* (50):158-168.
775 Deb, K. 2001. Multi-objective optimization using evolutionary algorithms (Vol. 16). John Wiley
776 & Sons.
777 Elofsson, K. 2003. Cost-effective Reductions of Stochastic Agricultural Loads to the Baltic
778 Sea. *Ecological Economics*, 47(1):13-31.
779 Efron, B. 1979. Bootstrap methods: another look at the jackknife. *The annals of Statistics*, 1-26.
780 Evans-White, M. A., B.E. Haggard, and J.T. Scott. 2013. A Review of Stream Nutrient Criteria
781 Development in the United States. *Journal of Environmental Quality*, *42*(4):1002-1014.

Gramig, B. M., C. J. Reeling, R. Cibin, and I. Chaubey. 2013. Environmental and Economic Trade-offs in a Watershed when Using Corn Stover for Bioenergy. *Environmental Science & Technology*, *47*(4): 1784-1791.

Gren, M. 2010. Resilience Value of Constructed Coastal Wetlands for Combating Eutrophication. *Ocean & Coastal Management, 53*(7): 358-365.

Gren, M. 2008. Adaptation and Mitigation Strategies for Controlling Stochastic Water Pollution: An Application to the Baltic Sea. *Ecological Economics 66*(2): 337-347.

Gren, M., G. Destouni, and R. Tempone. 2002. Cost Effective Policies for Alternative Distributions of Stochastic Water Pollution. *Journal of Environmental Management, 66*(2): 145-157.Gassman, P. W. 2008. *A simulation assessment of the Boone River watershed: Baseline calibration/validation results and issues, and future research needs*. ProQuest

Goel, T. and N. Stander .2010. A non-dominance-based online stopping criterion for multi-objective evolutionary algorithms. *International Journal for Numerical Methods in Engineering, 84*(6), 661-684.

Heal, G., G. C. Daily,P.R.Ehrlich, J.Salzman, C.Boggs, J.Hellrnan,,and T. Ricketts. 2001 Protecting Natural Capital Through Ecosystem Service Districts. *Stanford Environmental Law Journal*, *20*, 333.

Heal, G. M. and A. A. Small. 2002. Agriculture and Ecosystem Services. *Handbook of Agricultural economics* (2):1341.

Herman, J. D., H.B. Zeff, P.M. Reed, and G.W. Characklis. 2014. Beyond Optimality: Multistakeholder Robustness Tradeoffs for Regional Water Portfolio Planning under Deep Uncertainty. *Water Resources Research 50*(10): 7692-7713.

Heiskary, S. A., R.W. Bouchard Jr. 2015. Development of Eutrophication Criteria for Minnesota Streams and Rivers using Multiple Lines of Evidence. *Freshwater Science*, *34*(2).

Hong, L. J., Y. Yang, and L. Zhang. 2011. Sequential Convex Approximations to Joint Chance Constrained Programs: A Monte Carlo Approach. *Operations Research 59*(3): 617-630.

Horan, R. D. and J.S. Shortle. 2011. Economic and Ecological Rules for Water Quality Trading. *JAWRA Journal of the American Water Resources Association*, *47*(1): 59-69.

Kampas, A. and B. White. 2003. Probabilistic Programming for Nitrate Pollution Control: Comparing Different Probabilistic Constraint Approximations. *European Journal of Operational Research*, *147*(1): 217-228.

Kampas, A. and K. Adamidis. 2005. Discussion of the paper "Cost Effective Policies for Alternative Distributions of Stochastic Water Pollution" by Gren, Destouni and Tempone. *Journal of Environmental Management*, *74*(4): 383-388.

Karp, D. S., C.D. Mendenhall, E. Callaway, L.O. Frishkoff, P.M. Kareiva, P. R. Ehrlich, and G.C. Daily. 2015. Confronting and Resolving Competing Values behind Conservation Objectives. *Proceedings of the National Academy of Sciences*, *112*(35): 11132-11137.

Kennedy, M. C., E.D. Ford, P. Singleton, M. Finney, and J.K. Agee. 2008. Informed Multi-Objective Decision-Making in Environmental Management using Pareto Optimality. *Journal of Applied Ecology 45*(1): 181-192.

Kling, C. L. 2011. Economic Incentives to Improve Water Quality in Agricultural Landscapes: Some New Variations on Old Ideas. *American Journal of Agricultural Economics*, *93*(2): 297-309

827 Kurkalova, L. A. 2005. Carbon Sequestration in Agricultural Soils: Discounting for
828 ncertainty. *Canadian Journal of Agricultural Economics/Revue canadienne*
829 *d'agroeconomie 53*(4): 375-384
830 Lankoski, J. and M. Ollikainen. 2003. Agri-environmental Externalities: A Framework for
831 Designing Targeted Policies. *European Review of Agricultural Economics 30*(1):51-75.
832 Lichtenberg, E. 2002. Agriculture and the Environment. *Handbook of Agricultural*
833 *Economics, 2:* 1249-1313.
834 Lichtenberg, E. and D. Zilberman. 1988. Efficient Regulation of Environmental Health
835 Risks. *The Quarterly Journal of Economics* (89): 167-178.
836 Longstaff, P. H., T.G. Koslowski, and W. Geoghegan. 2013. Translating Resilience: A
837 Framework to Enhance Communication and Implementation. In *Symposium on Resilience*
838 *Engineering* (pp. 12-23).
839 Maier, H. R., Z. Kapelan, J. Kasprzyk, J. Kollat, L.S. Matott, M. C. Cunha, and P.M. Reed.
840 2014. Evolutionary Algorithms and other Metaheuristics in Water Resources: Current Status,
841 Research Challenges and Future Directions. *Environmental Modelling & Software, 62*:271-299.
842 McSweeny, W. T. and J.S. Shortle. 1990. Probabilistic Cost Effectiveness in Agricultural
843 Nonpoint Pollution Control. *Southern Journal of Agricultural Economics 22*(1): 95-104.
844 Mueller, N. D., E.E. Butler, K. A. McKinnon, A. Rhines, M. Tingley, N.M., Holbrook, and P.
845 Huybers. 2015. Cooling of US Midwest Summer Temperature Extremes from Cropland
846 Intensification. *Nature Climate Change*.
847 Muller, N. Z., R. Mendelsohn, and W. Nordhaus. 2011. Environmental Accounting for Pollution
848 in the United States Economy. *The American Economic Review*, 1649-1675.
849 Nicklow, J., P. Reed, D. Savic, T. Dessalegne, L, Harrell, A. Chan-Hilton, M. Karamouz et al.
850 "State of the art for genetic algorithms and beyond in water resources planning and

management." *Journal of Water Resources Planning and Management* 136, no. 4 (2009): 412-432.

Paris, Q. 1979. Revenue and Cost Uncertainty, Generalized Mean-variance, and the linear complementarity problem. *American Journal of Agricultural Economics*, *61*(2), 268-275.

Parkhurst, G. M., and J.F. Shogren, J. F. 2007. Spatial Incentives to Coordinate Contiguous Habitat. *Ecological Economics*, *64*(2): 344-355.

Polasky, S. and K. Segerson. 2009. Integrating Ecology and Economics in the Study of Ecosystem Services: Some Lessons Learned. *Annual Review of Resource Economics* 1: 409-434.

Polasky, S., E. Nelson J. Camm, B. Csuti, P. Fackler, E. Lonsdorf, and C. Tobalske. 2008. Where to Put Things? Spatial Land Management to Sustain Biodiversity and Economic Returns *Biological Conservation 141*(6): 1505-1524.

Politis, D. N. and J.P. Romano. 1992. A circular block-resampling procedure for stationary data. *Exploring the limits of bootstrap*, 263-270.

Politis, D. N. and J.P. Romano.1994. The stationary bootstrap. *Journal of the American Statistical association*, *89*(428), 1303-1313.

Poojari, C. A., and Varghese, B. (2008). Genetic algorithm based technique for solving chance constrained problems. *European journal of operational research,185*(3), 1128-1154.

Porto, M. and O. Correia and P. Beja. 2014. Optimization of Landscape Services under Uncoordinated Management by Multiple Landowners.

Prekopa, A. 1970. On Probabilistic Constrained Programming. In *Proceedings of the Princeton Symposium on Mathematical Programming* (pp. 113-138). Princeton, NJ: Princeton University Press.

874 *Proceedings of the National Academy of Sciences*,
875 http://www.pnas.org/cgi/collection/nature_capital
876 Rabotyagov, S. S. (2010). Ecosystem Services under Benefit and Cost Uncertainty: An
877 Application to Soil Carbon Sequestration. *Land Economics 86*(4): 668-686.

878 Rabotyagov, S. S., M. Jha, and T.D. Campbell. 2010. Nonpoint-Source Pollution Reduction for
879 an Iowa Watershed: An Application of Evolutionary Algorithms. *Canadian Journal of*
880 *Agricultural Economics/Revue canadienne d'agroeconomie*, *58*(4): 411-431.

881 Rabotyagov, S. S., T. D. Campbell, M. White, J.G. Arnold, J. Atwood, M. L.Norfleet, C.L. Kling
882 et al. "Cost-effective targeting of conservation investments to reduce the northern Gulf of
883 Mexico hypoxic zone." *Proceedings of the National Academy of Sciences* 111, no. 52 (2014):
884 18530-18535.

885 Roy, A. D. 1952. Safety First and the Holding of Assets. *Econometrica* 431-449.

886 Shortle, J. and R.D. Horan. 2013. Policy Instruments for Water Quality Protection. *Annu. Rev.*
887 *Resour. Econ.*, *5*(1): 111-138

888 Steffen, W., K. Richardson, J. Rockström, S.E. Cornell, I. Fetzer, E.M. Bennett, and S. Sorlin.
889 2015. Planetary Boundaries: Guiding Human Development on a Changing
890 Planet. *Science*, *347*(6223): 1259855.

891 Tóth, S. F. and M.E. McDill. 2009. Finding Efficient Harvest Schedules under Three Conflicting
892 Objectives. *Forest Science* 55(2): 117-131.

893 USDA-CEAP, Wildlife National Assessment. 2015.
894 http://www.nrcs.usda.gov/wps/portal/nrcs/detailfull/national/technical/nra/ceap/na/?cid=nrcs143
895 _014151

US EPA, 2015 http://www2.epa.gov/nutrientpollutionWillis, D. B. and N.K. Whittlesey. 1998. The Effect of Stochastic Irrigation Demands and Surface Water Supplies on On-Farm Water Management. *Journal of Agricultural and Resource Economics* 206-224.

Zitzler, E., M. Laumanns, and L.Thiele.2002. "Spea2: Improving the strength pareto evolutionary algorithm for multiobjective optimization." *Evolutionary Methods for Design, Optimization, and Control* (2002): 95-100.

Appendix 1

As noted in the text, a solution to the chance-constrained problem (3) must be a member of the Pareto frontier in the cost-mean-standard deviation space: $\hat{\mathbf{x}} \subset \mathbf{x}^*$. The converse is not true: that is, a particular solution from a multiobjective optimization program need not be optimal for a chance-constraint program. Obtaining a Pareto-frontier (and a mean-variance frontier) is, in principle, more general, and the specific weight placed on the standard deviation determines the point of "tangency" between the efficient frontier and the "α-isoresilient" pollution load line of form $E_T\{\mathrm{N}(\hat{\mathbf{x}})\} + \phi^{\alpha} Var(N(\hat{\mathbf{x}}))_T^{0.5} \equiv N(\alpha)$. Figure 1 graphically depicts this point. For a particular weight ϕ^{α} placed on the standard deviation, point A in the Pareto-frontier would be optimal, while point B would appear to be suboptimal given ϕ^{α}. However, for a different reliability requirement associated with a lower probability of reaching pollution reduction goal, point B would be optimal. These considerations require us to "post-process" the simulated Pareto-frontier when they are collapsed to "resilient" pollution quantities to eliminate original members of the mean-variance efficient frontiers which appear dominated given a specific distributional assumption or the desired level of resilience. By construction, any nitrogen load level equal to $N(\alpha)$ is achieved with probability α.

943 Figure A1: Pareto frontier and mean-variance minimums

944

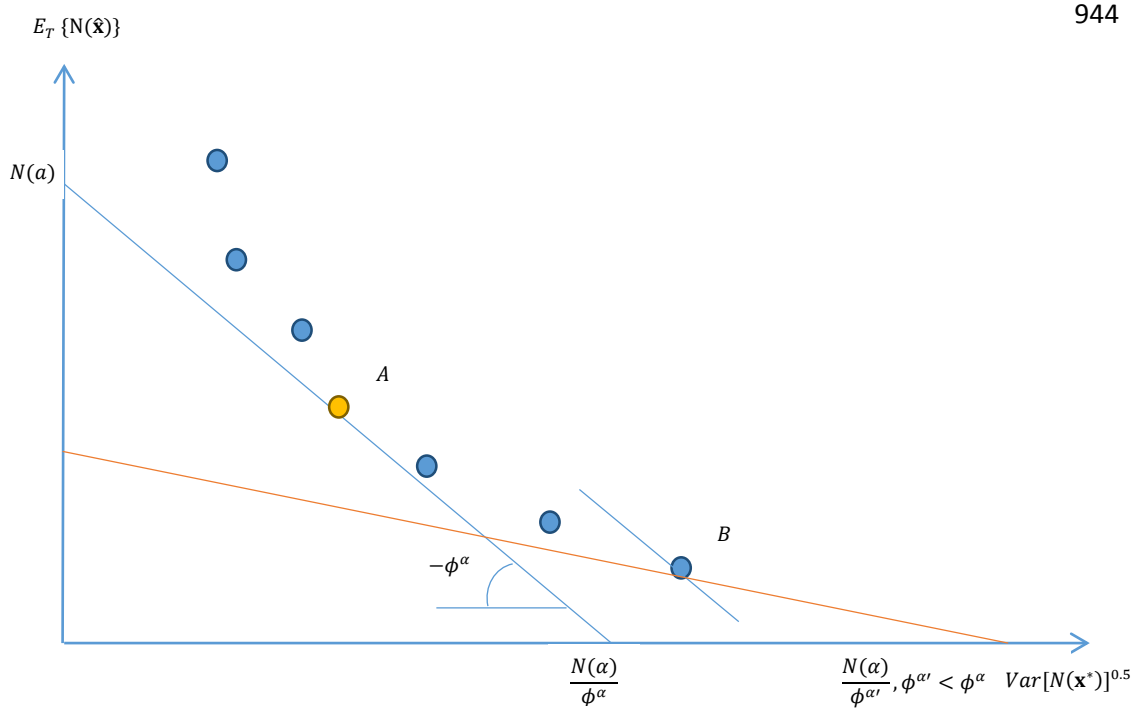

945 Figure A2 The Pareto frontrier: Cost-Mean-Standard deviation

946

947

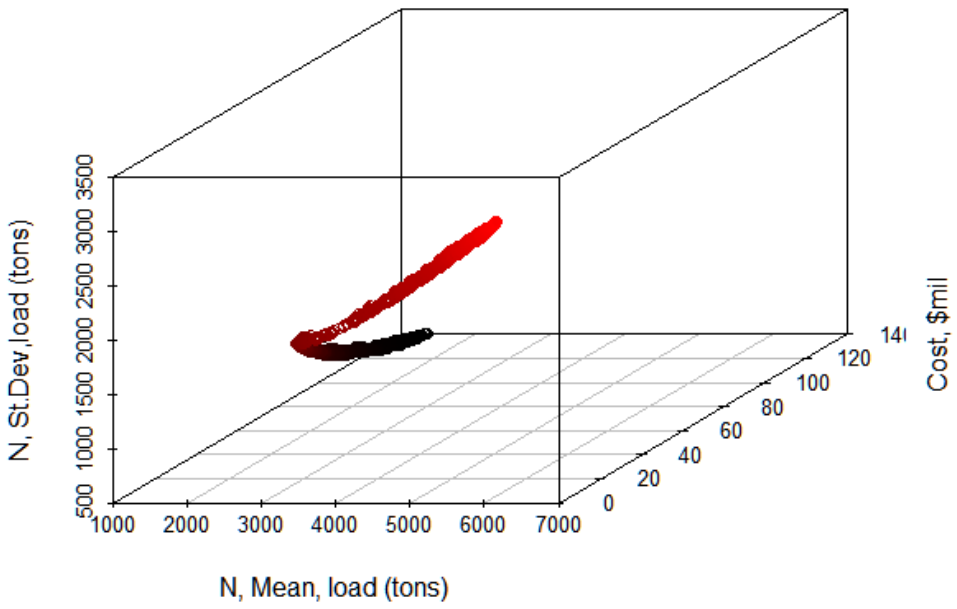

948

949

Figure A3: Distribution of Conservation Practices

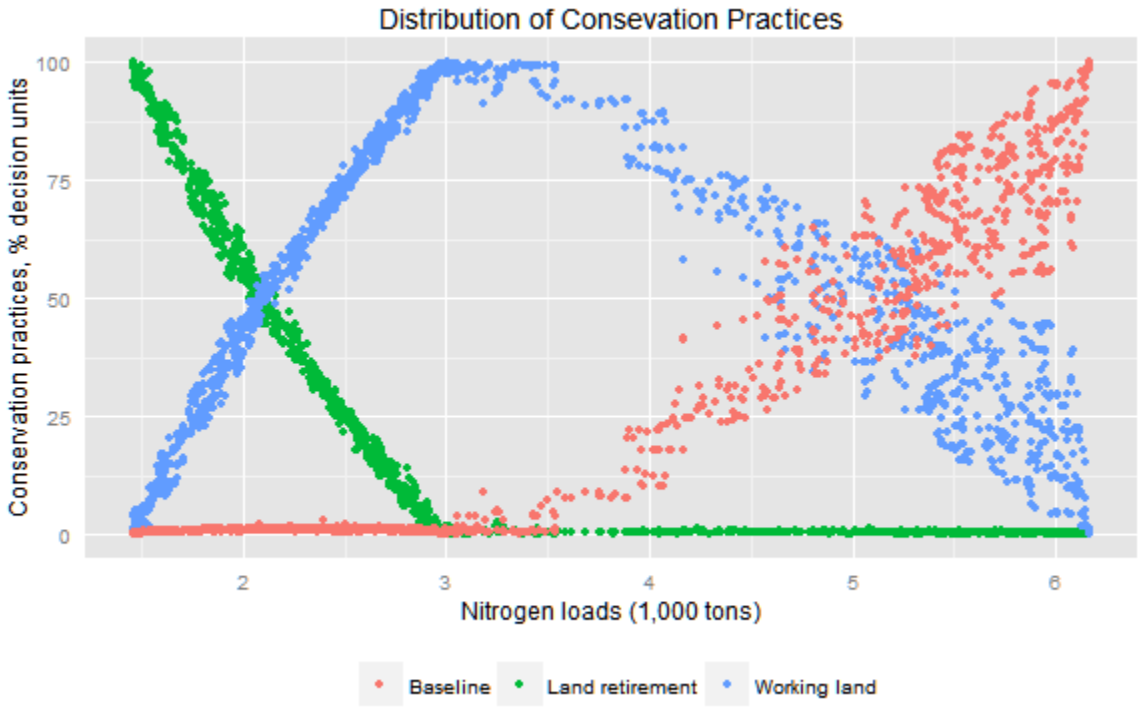

Figure A3 shows the distribution of conservation practices across the entire set of Pareto-efficient solutions expressed as the percentage of the number of decision-making units ("fields") selected to a type of conservation practice.[13]

We group cover crops, no-till and their combination into a single category labeled as "Working Land". "Baseline" represents the case where no action is taken, and "Land Retirement" considers taking land out of agricultural production. As expected, lower levels of nutrient loads can be achieved by placing land in land retirement, and larger loads correspond to using "Working Land" conservation actions.

[13] The decision-making unit in the analysis is an HRU, or a Hydrologic Response Unit (see Gassman, 2008).

The three groups each display an inflection point that corresponds approximatively to the same level of emissions. Hence, the steeper part in Figure 1(b) can be explained by the decline in the use of “Land Retirement”; the smoother decreasing part is explained by the decline in ”Working Land”, while the relatively flat area is explained by the increase in the baseline. These trends suggest that land retirement leads to lower variation in N pollution and targets with higher resilience will require using it extensively (following Gren 2010, one can say that land retirement possesses “resilience value” with respect to nutrient reductions). Similar variation-reducing properties of simulating land retirement were reported in Rabotyagov, Jha, and Campbell (2010). The inflection point can be also explained by the limited effectiveness of the “working land” practices considered in reducing N and by the fact that “Land Retirement” is the most effective conservation practice. The inflection point corresponds to a low level of emissions (high level of targets), where steep increases in land retirement are needed to attain those expected reductions in N.

Figure A4 Comparison α-resilient Pareto Frontiers

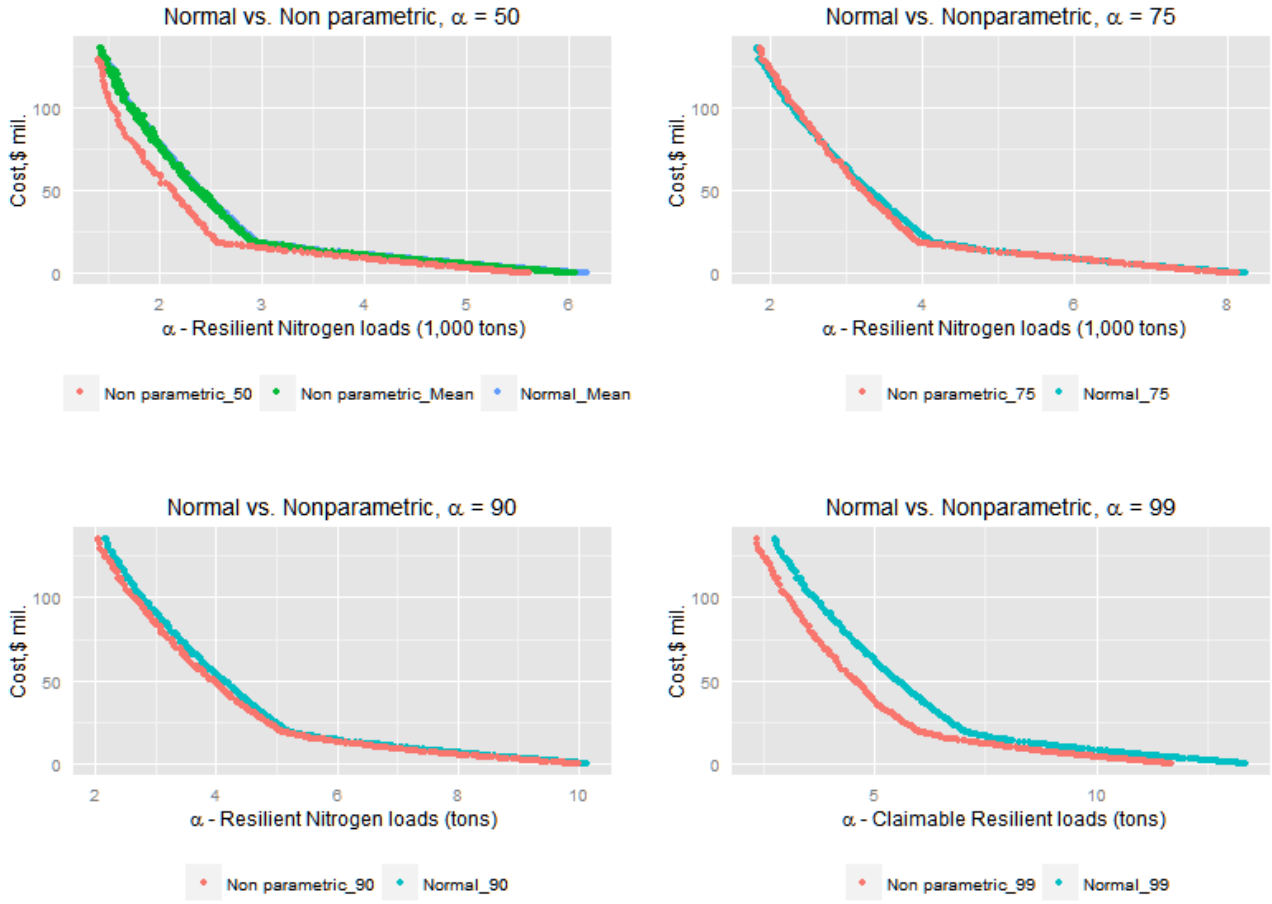

Figure A5 Cost-Resilience Trade-offs

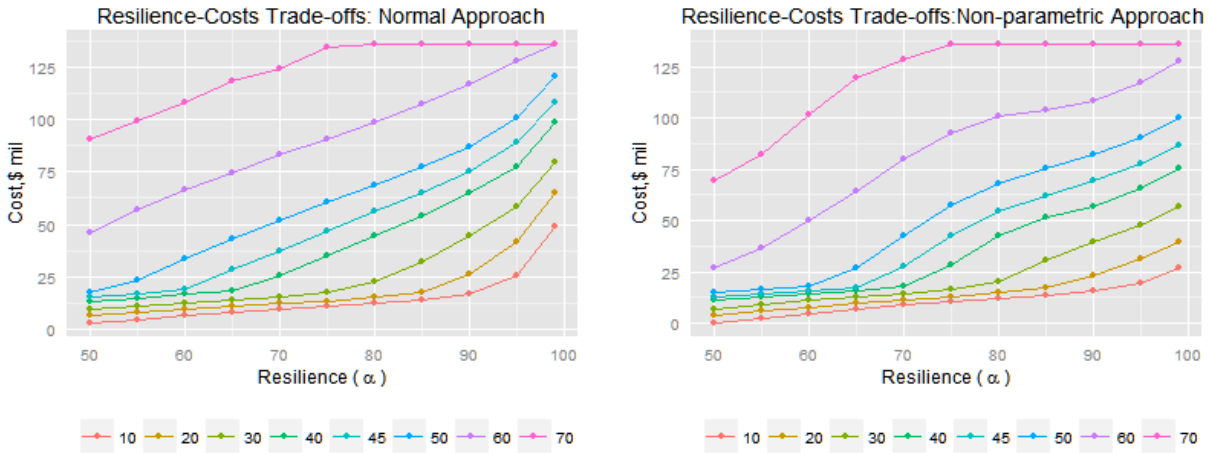

Figure A4 compares pairwise the resilient Pareto frontiers under the two approaches. The comparisons suggest that the non-parametric distribution has lighter tails than the normal distribution. This difference suggests that for a very large resilience (99), the critical value for standard normal is too conservative relative to the corresponding bootstrapped quantile. Figure A5 summarizes the resilience - cost trade-offs for achieving the same level of resilient N loads. We define a set of eight nitrogen load targets ($\overline{N}$,) each corresponding to reductions in the historical loads ranging from 10 percent to 70 percent.

988 Figure A6 Resilience-Nitrogen-Phosphorus Trade-offs

989

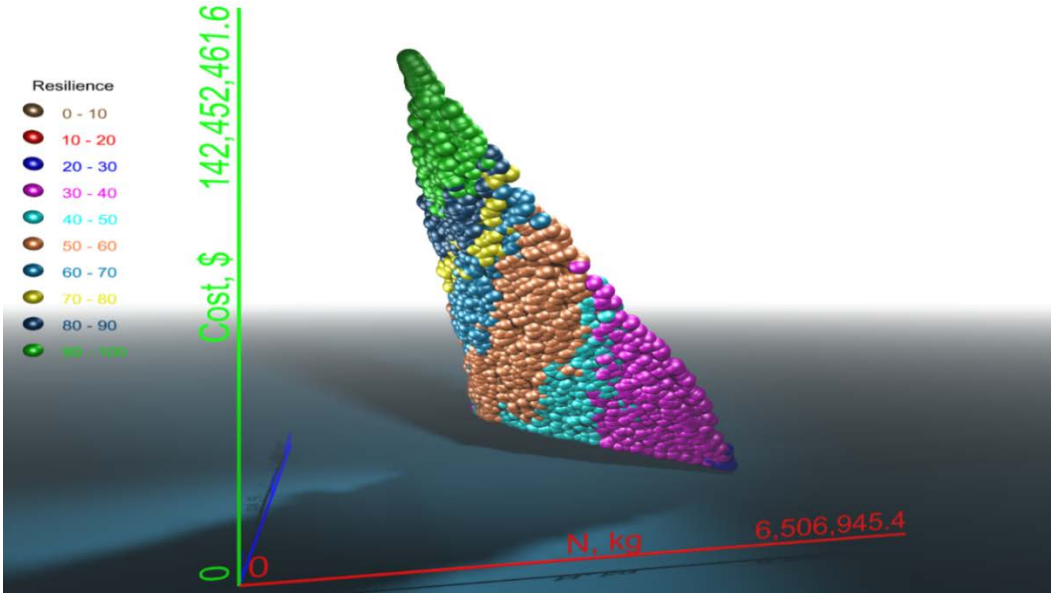

990

991 A three dimension illustration of this tradeoffs when the targets are set equal to 45
992 percent reductions for both N and P (equation 9) is presented in the supplemental material
993 (Figure A6). Each element on this frontier (a 3-dimensional projection of the 5-dimensional
994 Pareto-frontier P_f^{NP}) is assessed for a resilience (probability) level of achieving this joint target.
995 As for the single pollutant case: securing higher level of resilience demands higher costs.
996 Furthermore, the elements in the upper part of the curve (green colored) have the highest level of
997 resilience (higher than 90 percent) but at the same time they have the highest total costs. From
998 Figure 10, one can see that for a particular interval of joint resilience, there is more than one
999 solution on the frontier. Thus, it is likely, that for a particular level of simulated joint resilience,
1000 multiple solutions would be present (for example, both a solution which over-reduces N but just
1001 reduces P to satisfy the desired P-resilience and a solution that just satisfies the criterion of joint
1002 resilience would be present). Figure A7 summarizes the results of this kind of phenomenon for

ten levels of joint resilience. Note the similarity to considerations discussed in connection with figure 1.

Figure A7 Cost of Resilience under Joint Target

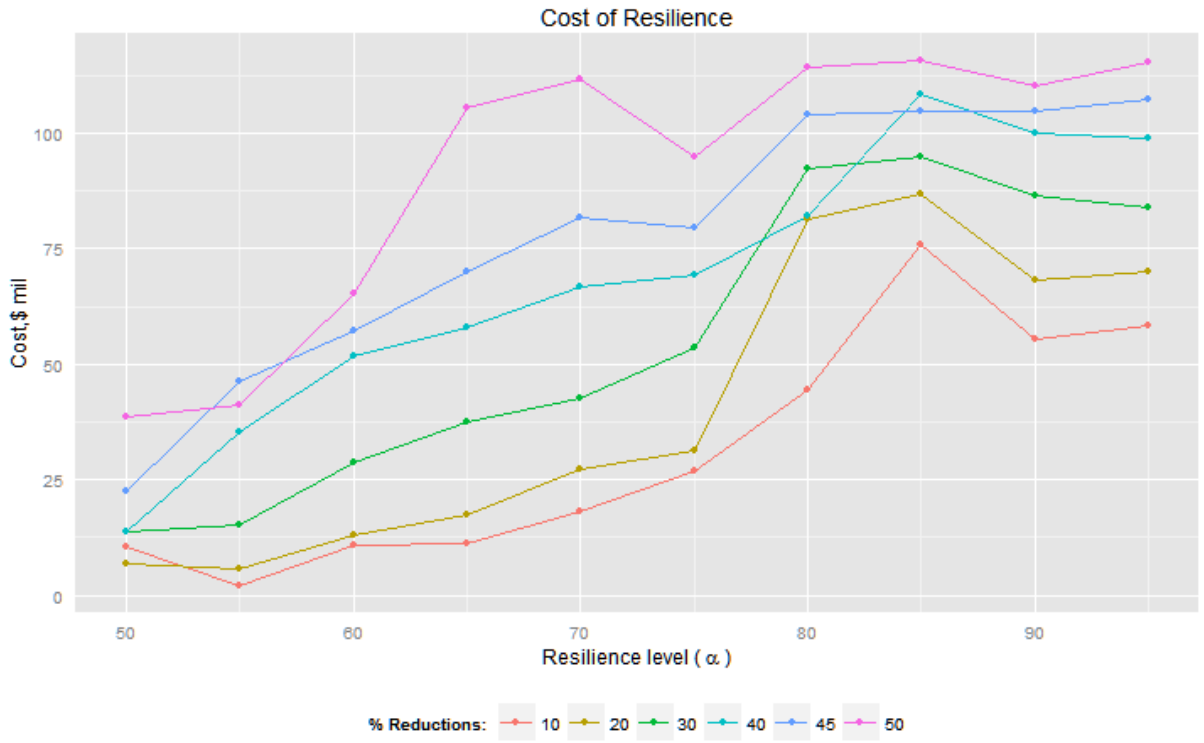

Figure A7 depicts the cost curves associated with the set of joint resilient targets. As in the single pollutant case, these curves are mostly increasing, although some of the cost curves for less stringent targets cross the cost curves for more restrictive targets, although the overlaps take place in the range of higher resilient levels. This behavior is a manifestation of inefficiencies present in the overall tradeoff frontier when evaluated from a point of view of specific nutrient reductions and their joint resilience. We conjecture that developing tailored algorithms associated with each of the lines presented would a) restore the ranking of the curves and eliminate the overlap and b) would eliminate the spikes in individual curves and therefore negative marginal costs of additional resilience.

Figure A8 Spatial Distribution of Conservation Practices in the Watershed.

A shown by our empirical findings, the distribution of conservation practices differs across resilience level. This implies that the spatial distribution will be very different. The next figures show the spatial placement of conservation practices when the target is set to 45 percent reductions and for three resilience levels: 50, 75, and 99.

Figure A8 depicts the spatial placement of the conservation practices in the watershed when the target is set equal to 45 percent reductions for N only and for joint N and P for three resilience levels: 50,75, and 99. The watershed configurations reinforce the previous findings: higher resilience levels require extensive use of land retirement, with more land retirement being used when both N and P are targeted. The non-parametric and normal watershed configurations are very similar when resilience levels are 50 or 75. However, the normal 99 resilience configuration has higher use of land retirement. This confirms the fact that the 99^{th} quantile value for the standard normal is too conservative relative to the non-parametric quantile.

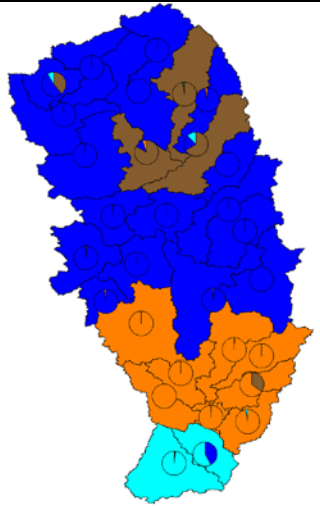 $\alpha = 50$ Non Parametric	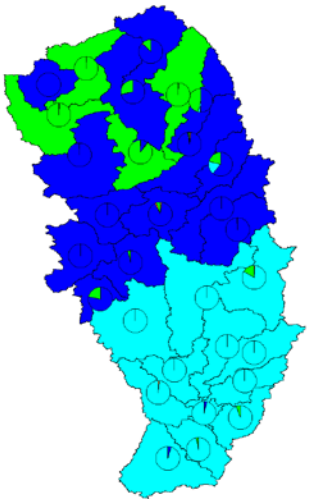 $\alpha = 75$ Non Parametric	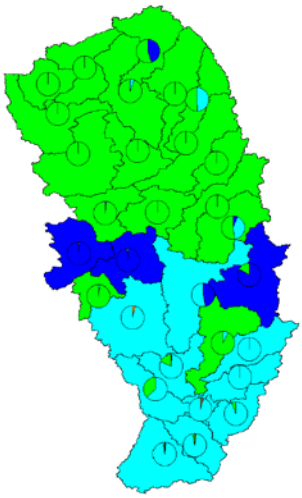 $\alpha = 99$ Non Parametric	
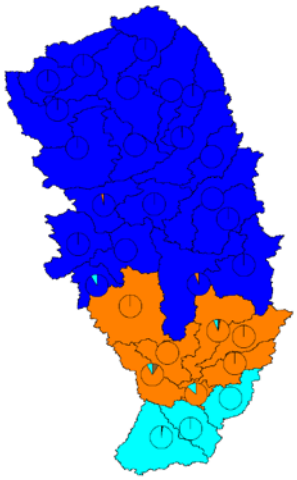 $\alpha = 50$ Normal	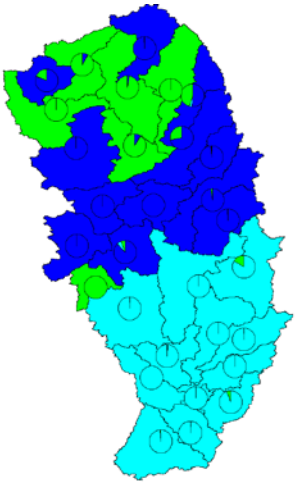 $\alpha = 75$ Normal	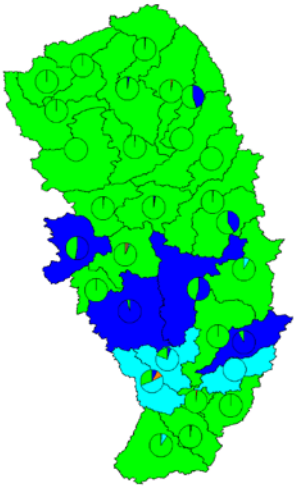 $\alpha = 99$ Normal	
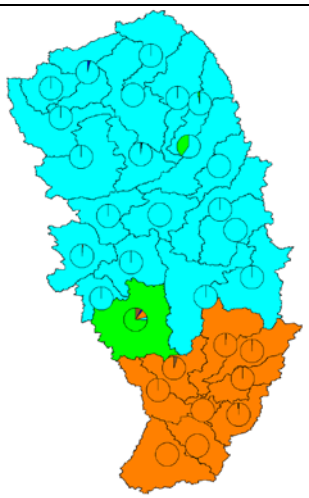 $\alpha = 50$ N and P	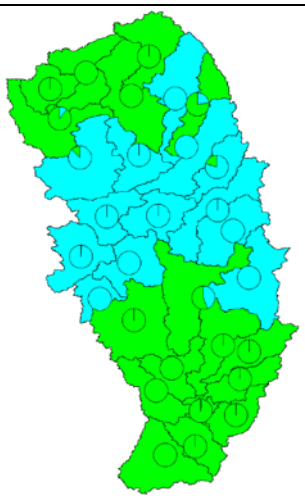 $\alpha = 75$ N and P	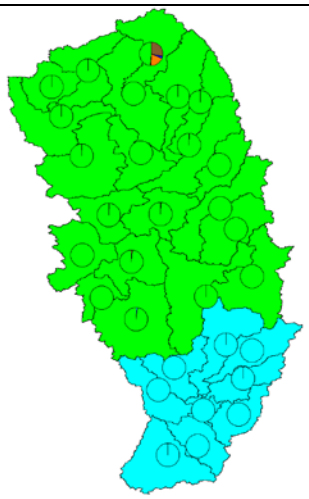 $\alpha = 99$ N and P	

Brown: Baseline; Orange: No-till; Blue: Cover Crops, Light Blue: Cover Crop and No-till, Green: Land Retirement. The main color represents the dominant color at sub-basin level. The pie charts represent percentage use for the entire set of practices[14].

[14] There are 2122 HRUs (*K* decision units). They are grouped in thirty sub-basins.

Table A1 Cost-Resilient Solutions; N reductions = 45% (target N=3.39 thousand tons N)

Resilience(α, %)	Cost (mil. $)	Marginal Cost (mil. $)	Working Land (%)	Land Retirement (%)	Baseline (%)	Cost (mil. $)	Marginal Cost (mil. $)	Working Land (%)	Land Retirement (%)	Baseline (%)
	Non-parametric					Normal				
50	12.94	0.00	91.70	0.50	7.90	15.16	0.00	99.20	0.20	0.60
55	14.47	1.52	99.20	0.20	0.60	17.08	1.92	98.30	1.00	0.80
60	16.04	1.57	96.70	0.30	3.00	19.25	2.17	98.90	0.60	0.50
65	17.61	1.57	97.90	0.20	1.90	28.36	9.11	89.80	9.50	0.80
70	27.47	9.86	93.10	5.90	1.00	37.21	8.85	78.80	20.00	1.20
75	42.40	14.93	75.50	23.20	1.20	46.89	9.68	71.40	28.00	0.60
80	54.38	11.99	63.10	35.90	1.00	56.39	9.50	64.10	35.10	0.80
85	62.06	7.68	54.40	44.60	0.90	65.27	8.88	54.90	44.20	0.90
90	69.76	7.70	48.60	50.20	1.20	75.43	10.16	44.70	54.10	1.30
95	77.54	7.78	41.20	57.80	0.90	88.93	13.50	31.50	67.60	0.90
99	86.99	9.45	40.80	58.40	0.80	107.96	19.03	17.80	81.60	0.60

Table A1 describes in detail the cost-resilient solutions for achieving the three levels of claimable nitrogen reductions for increments of about five percent increase in the resilience level from 50 to 99 probability levels for the two approaches. Column 1 shows the resilience levels α; and subsequent columns show the annual costs for achieving the required resilient loads for each level of resilience (million $), the marginal cost of achieving each additional level of resilience (million $). The following columns describe the distribution of the conservations practices: working land, land retirement and baseline (percentages of total decision-making units). We focus our analysis for case where the target is set equal to 45 percent reductions. . Resilience

levels lower than 70 percent are characterized by high use of working land conservation practices (higher than 93 percent). In order to secure higher levels of resilience more land is allocated to land retirement, but the increase takes place at a decreasing rate. For example, the use of land retirement increases from 5.9 percent (resilience level 70) to 23.2 percent (resilience level 75) (i.e. a total increase of 17 percent), but it takes only 6 additional percent to move for a resilience level of 85 to 90.

Next, we compare the costs and distribution of the conservation practices when the target is set at 45 percent reductions using normal approach with the ones described above. The total costs under the normal approach are slightly higher than under the non-parametric approach ranging from 15.94 to 107.96 million per year across different level of resilience. Lower levels of resilience are achieved by using working land conservation on a large number of fields (higher than 98 percent). Similarly, securing higher level of resilience requires putting more land in land retirement, but the use of land retirement increases at an increasing rather than decreasing rate. The increasing factor also explains the increasing trends in the marginal costs. Additionally, the optimal resilient loads ($N(\alpha)$) are a bit higher (less reductions) under the normal approach.

Table A2 Cost of Joint Resilience, 45% Reduction Target in N and P (N=3.39 thousand tons, P=0.09 thousand tons)

Resilience (α, %)	Cost (mil. $)	Marginal Cost (mil. $)	Working Land (%)	Land Retirement (%)	Baseline (%)
50	22.39	0.00	97.64	1.23	1.13
55	46.23	23.84	71.58	26.20	2.21
60	57.18	10.95	62.16	36.66	1.18
65	69.96	12.78	54.71	42.27	3.02
70	81.67	11.72	37.23	59.38	3.39
75	79.54	-2.13	44.16	55.75	0.09
80	103.92	24.37	22.48	76.34	1.18
85	104.99	1.07	21.54	77.43	1.04
90	104.72	-0.27	23.61	75.59	0.80
95	107.38	2.67	29.59	69.70	0.71

1079

1080